Toxicology in Vitro 61 (2019) 104610

Contents lists available at ScienceDirect

Toxicology in Vitro

journal homepage: www.elsevier.com/locate/toxinvit

Multi-endpoint toxicological assessment of polystyrene nano- and microparticles in different biological models *in vitro*

Michelle Hesler[a,1], Leonie Aengenheister[b,1], Bernhard Ellinger[c], Roland Drexel[d], Susanne Straskraba[e], Carsten Jost[f], Sylvia Wagner[a], Florian Meier[d], Hagen von Briesen[a], Claudia Büchel[e], Peter Wick[b], Tina Buerki-Thurnherr[b], Yvonne Kohl[1,*]

[a] Fraunhofer Institute for Biomedical Engineering IBMT, Joseph-von-Fraunhofer-Weg 1, 66280 Sulzbach, Germany
[b] Particles-Biology Interactions, Empa, Swiss Federal Laboratories for Materials Science and Technology, Lerchenfeldstrasse 5, 9014 St. Gallen, Switzerland
[c] Branch Lab ScreeningPort of the Fraunhofer Institute for Molecular Biology and Applied Ecology IME, Schnackenburgallee 114, 22525 Hamburg, Germany
[d] Postnova Analytics GmbH, Max-Planck-Straße 14, 86899 Landsberg am Lech, Germany
[e] Goethe University Frankfurt, Institute for Molecular Bioscience, Max-von-Laue-Straße 9, 60438 Frankfurt am Main, Germany
[f] PlasmaChem GmbH, Schwarzschildstraße 10, 12489 Berlin, Germany

ARTICLE INFO

Keywords:
Nano- and microplastics
Polystyrene
Multi-endpoint toxicity study
Intestinal barrier
Placental barrier
Embryotoxicity

ABSTRACT

Nanoplastics (NP) and microplastics (MP) accumulate in our environment as a consequence of the massive consumption of plastics. Huge knowledge-gaps exist regarding uptake and fate of plastic particles in micro- and nano-dimensions in humans as well as on their impact on human health.

This study investigated the transport and effects of 50 nm and 0.5 µm COOH-modified polystyrene (PS) particles, as representatives for NP and MP, in different biological models *in vitro*. Acute toxicity and potential translocation of the particles were studied at the human intestinal and placental barrier using advanced *in vitro* co-culture models. Furthermore, embryotoxicity and genotoxicity were investigated as highly sensitive endpoints.

Polystyrene was not acutely toxic in both sizes (nano- and microparticles). No transport across the intestinal and placental barrier but a cellular uptake and intracellular accumulation of PS nano- and microparticles were determined. The particles were identified as weak embryotoxic and non-genotoxic.

In contrast to single-organ studies, this multi-endpoint study is providing a data-set with the exact same type of particles to compare organ-specific outcomes. Our study clearly shows the need to investigate other types of plastics as well as towards long-term or chronic effects of plastic particles in different biological models *in vitro*.

1. Introduction

Plastics consist of synthetic polymer materials. The first fully synthetic plastic, bakelite, was produced in 1909. While natural polymers such as deoxyribonucleic acid (DNA), ribonucleic acid (RNA), starch (amylose), or cellulose largely define our lives, their synthetic counterparts become more and more an environmental burden. Once released into the ecosystem as plastic waste, these materials remain for decades in the environment due to their persistence against environmental factors (Cole et al., 2011).

Since the start of mass production of plastics in the 1950s, the output has increased annually (Geyer et al., 2017). While in the 1950s around 1.5 million tons were produced, the amount has increased 200-fold to 299 million tons worldwide in 2013 (PlasticsEurope, 2015) and from the years 2015 to 2016 from 322 to 335 million tons a year, respectively (Consultic et al., 2016; PlasticsEurope, 2017, 2015). It is estimated that the quantities could double in the coming years (Jambeck et al., 2015). Around 90% of the total amount of plastics consists of the commonly used polymers high-density polyethylene (HDPE), low-density polyethylene (LDPE), polyvinyl chloride (PVC),

* Corresponding author.
E-mail addresses: michelle.hesler@ibmt.fraunhofer.de (M. Hesler), leonie.aengenheister@empa.ch (L. Aengenheister), bernhard.ellinger@ime.fraunhofer.de (B. Ellinger), roland.drexel@postnova.com (R. Drexel), susanne.straskraba@bio.uni-frankfurt.de (S. Straskraba), c.jost@plasmachem.com (C. Jost), sylvia.wagner@ibmt.fraunhofer.de (S. Wagner), florian.meier@postnova.com (F. Meier), hagen.briesen@ibmt.fraunhofer.de (H. von Briesen), peter.wick@empa.ch (P. Wick), tina.buerki@empa.ch (T. Buerki-Thurnherr), yvonne.kohl@ibmt.fraunhofer.de (Y. Kohl).
[1] These authors contributed equally to this work.

https://doi.org/10.1016/j.tiv.2019.104610
Received 13 May 2019; Received in revised form 16 July 2019; Accepted 24 July 2019
Available online 27 July 2019

polystyrene (PS), polypropylene (PP) and polyethylene terephthalate (PET) (Li et al., 2016). Two ways exist for the release of small plastic particles in the environment, whereby nanoplastics (NP) is usually included in the terminology of microplastics (MP): as primary plastics released from MP containing products or as secondary MP, which are created due to degradation or ageing processes of plastic fragments triggered by sunlight and other environmental influences (Ivar do Sul and Costa, 2014; Wright et al., 2013).

Only few data are available dealing with the appearances and shapes of secondary MP in the environment (Burns and Boxall, 2018). Recent laboratory studies investigated the fragmentation of PS objects like coffee cup lids, single-use plates and PS foams in the environment by simulating the degradation process with UV-light radiation (Lambert and Wagner, 2016) or mechanical fragmentation in the sea swash zone with bottom sediments in a rotating mixer (Efimova et al., 2018). Ekvall et al. explored the formation of NP during the mechanical breakdown of daily-use PS products like coffee cup lids and expanded PS foam (Ekvall et al., 2019). All these studies demonstrated that PS NP and MP are actually formed in the environment and appear in spherical shapes in various sizes, especially when foamed PS is degraded (Efimova et al., 2018). Tanaka and Takada (2016) identified spherical PS microbeads in digestive tracts of fish collected from urban coastal waters (Tanaka and Takada, 2016). Furthermore, due to the photo-initiated oxidative degradation of PS in the environment, carboxylic end groups are formed on the MP surface (Gewert et al., 2015).

PS, also known as styrofoam (expanded PS) and used as insulation and packaging material, is also present in various areas of daily use. Primary MP are produced by industry, for example, as additives in personal care and cosmetic products (PCCPs) or in detergents (Leslie, 2014; Plastic Soup Foundation, 2018; Shim et al., 2018) and are released into the environment upon use of these products (Holm et al., 2013). Since 500 tons of MP are manufactured per year in Germany for their use in PCCPs, this product group is regarded as a critical source of MP contamination (Miklos et al., 2016). Around 10% of the annual plastics production ends up in the oceans because of insufficient treatment capacity, accidental inputs, littering, illegal dumping and coastal human activities (Avio et al., 2017; Wang et al., 2016; Waring et al., 2018). Microparticles were not only found in the ocean (Avio et al., 2017; Gall and Thompson, 2015; Vroom et al., 2017). They are also present in lakes (Fischer et al., 2016; Klein et al., 2015; Lechner et al., 2014; Wang et al., 2017b; Blettler et al., 2017), and in Arctic sea ice of up to 12.000 particles per cubic meter (Kanhai et al., 2017; Lusher et al., 2015; Suaria et al., 2016; Woodall et al., 2014; Waller et al., 2017). Therefore, the EU Commission is considering a ban on MP in cosmetics, personal care, detergents and cleaning agents by 2020, so that in future dermal exposure can be neglected. Also, a strategy against plastic waste in the seas was presented by the EU at the end of May 2018 (European Commission, 2018). The persistence of plastic materials leads to their accumulations in so-called “garbage patches” in the oceans (Law and Thompson, 2014). This marine litter is a significant threat to the entire ecosystem since the ingestion and entanglement of macro-plastics end up in death for many marine species. But also, human health is at risk. MP have already been determined in numerous foods, such as fish (Bessa et al., 2018; Davidson and Dudas, 2016; Hermsen et al., 2017; Rummel et al., 2016), shrimp (Bessa et al., 2018), sardines (Karami et al., 2018), and mussels (Auta et al., 2017; EFSA, 2016a, 2016b; Van Cauwenberghe et al., 2015; Van Cauwenberghe and Janssen, 2014). MP were also detected in sea salt (Iñiguez et al., 2017; Karami et al., 2017; Yang et al., 2015), honey and sugar (Liebezeit and Liebezeit, 2013), beer (Kosuth et al., 2018; Liebezeit and Liebezeit, 2014) or tap water (Kosuth et al., 2018). Investigations of drinking water showed low levels of MP contamination (0.4–7 particles/m^3) (Mintenig et al., 2014). MP accumulate in the ground water (Holm et al., 2013; Lusher et al., 2017; Pörschke and Eloo, 2016) because it is not possible to filter all particles in sewage treatment plants due to their broad size range (< 0.1–5000 µm). In addition to oral exposure, humans may also inhale airborne MPs (*e.g.*, MP from car tire abrasion).

It is known that MP has numerous adverse effects on the ecosystem and environmental organisms (Huerta Lwanga et al., 2017; Luís et al., 2015; Rodriguez-Seijo et al., 2017; Watts et al., 2015, 2016), which classifies it as an environmental pollutant (Galloway et al., 2017). MP in various sizes (nano and micron size) can trigger different harmful effects in aquatic organisms including direct physical damage (tissue damage, accumulation, inflammation) and toxicity related to oxidative stress (Canesi et al., 2015; Sun et al., 2018). Effects caused from the release of pollutants which are deposited on the MP and are absorbed into the organisms are possible (Browne et al., 2013; Lusher et al., 2017; von Moos et al., 2012; Welden and Cowie, 2016; Wright and Kelly, 2017). Not only in aquatic, but also other organisms such as the mosquito (Culex mosquito), uptake and storage of the MP in the tissue was identified (Al-Jaibachi et al., 2019). Environmental pollutants often persist not only in the environment, but can also be transferred to humans.

Against this background, there is an urgent need for the human risk assessment of NP and MP. Until today only a limited number of studies exist on the absorption and transport behavior of NP or MP in the human body (EFSA, 2016a, 2016b; Lusher et al., 2017; Revel et al., 2018). NP and MP most likely enter the human organism *via* the food chain or through contamination of the respiratory air (Hussain et al., 2001; Lusher et al., 2017; Prata, 2018; Revel et al., 2018; Wright and Kelly, 2017). Since previous research has focused mainly on the aquatic environment, there are only few studies available on the contamination of terrestrial areas and the effect of MP in terrestrial animals and organisms at the end of the food web (Awet et al., 2018; Cuthbert et al., 2019; de Souza Machado et al., 2018; Huerta Lwanga et al., 2017).

A decisive factor for the uptake in the organism is the particle size. Particles < 150 µm can potentially be absorbed through the intestinal mucosa and pass to the lymphatic system, particles < 110 µm can enter the bloodstream through the portal vein and particles < 20 µm can reach internal organs (EFSA, 2016a, 2016b; Schmidt et al., 2013; Smith et al., 2018; Wright and Kelly, 2017). However, most of the orally ingested nanoparticles pass the gastrointestinal tract (GIT) without being absorbed over the GIT barrier (Kreyling et al., 2017). Crossing the intestinal barrier, particles < 100 nm can even be transported into the brain (Barboza et al., 2018; Betzer et al., 2017; Wright and Kelly, 2017) and across the placental barrier (Barboza et al., 2018; Betzer et al., 2017; Bouwmeester et al., 2015; Wick et al., 2010). Inhaled particles can be excreted by mucociliary clearance, but can also settle in the lungs or be absorbed into the bloodstream (Prata, 2018; Wright and Kelly, 2017). One hazard caused by MP is the formation of lesions and inflammations in the tissue. Oxidative stress, necrosis, and DNA damage can also be triggered (Lehner et al., 2019; Lusher et al., 2017). The few data which currently exist are contradictory, as there are also studies published, demonstrating that PS-nano- and -microparticles do not induce toxic effects (Ašmonaitė et al., 2018; Fröhlich et al., 2012; Loos et al., 2014; Wang et al., 2019).

Studies with polymeric particles applied as drug delivery systems showed cellular uptake of the particles in the human *in vitro* models Caco-2 and MDCK (Kulkarni and Feng, 2013) as well as the biodistribution *in vivo* (Hussain et al., 2001; Schmidt et al., 2013). But, very little is known about the toxicity caused by plastic particles following their uptake and the effect on human health. One *in vitro* study describes the induction of oxidative stress after the exposure of cerebral and epithelial human cells to PS-nano- and microparticles at a concentration of 10 mg/L (Schirinzi et al., 2017). There is an ongoing discussion on human health effects induced by plastic particles because too many questions are still open (Barboza et al., 2018).

To study nanosafety the selection of suitable proxies for NP and MP is strongly limited by the lack of suitable reference materials. To date, there are no standardized reference materials available, which would allow a reliable work with more realistic, random shaped or weathered particles (Hughes et al., 2015).

For this reason, in this study, the interaction and the translocation of PS-nanoparticles (50 nm) and PS-microparticles (0.5 µm) as representatives for NP and MP, were investigated in different biological models *in vitro*. Spherical carboxylated nano- and microparticles are present in the environment and can additionally be formed by degradation and fragmentation processes (Efimova et al., 2018; Ekvall et al., 2019; Gewert et al., 2015; Hughes et al., 2015; Isobe, 2016; Juliano and Magrini, 2017; Lambert and Wagner, 2016; Tanaka and Takada, 2016). Therefore, PS NP and MP frequently could also interact with the human organism.

In this study, two biological barriers were chosen to investigate the translocation and the intracellular distribution: the GI tract, as the most likely entry port of MP and NP and the placental barrier, covering the most vulnerable subpopulation, the fetus. To consider the toxic potential of PS-NP and –MP for the embryo, the embryonic stem cell test was performed as one sensitive endpoint of our multi-endpoint study. As the DNA damaging potential of NP and MP on human cells is an open question so far, genotoxicological investigations were performed additionally. In contrast to single-organ studies, the analysis of these multiple endpoints will provide a consistent data-set to assess the impact of the same material (nano- *vs* micron-sized) with the same surface charge on multiple human organs/tissues to allow for a direct comparison of the organ-specific outcomes. This study is an essential contribution to the toxicological assessment of PS nano- and microparticles.

2. Materials and methods

2.1. Synthesis and functionalization of the PS particles

PS nanoparticles were synthesized *via* emulsion polymerisation with styrene, acrylic acid, divinylbenzene as a cross-linker, sodium-dodecylbenzenesulfonate as stabiliser and rhodamine 6G as fluorescence marker as previously described (Awet et al., 2018). For surface functionalization acrylic acid was added to the reaction mixture, resulting in a carboxy-modified surface (PS-COOH). For PS microparticles, commercially available PS particles functionalized with carboxylic surface-groups have been used (PS-COOH-L2867, Microparticles GmbH, Berlin, Germany) introducing the fluorescence marker rhodamine 6G after activation with 1-Ethyl-3-(3-dimethylaminopropyl)carbodiimide (EDC). To evaluate the particle surface coverage with carboxylic groups, a titration with 0.01 M NaOH / 0.1 M NaCl was performed, controlled by a pH-measuring system.

2.2. Transmission electron microscopy (TEM)

Transmission electron microscopy (TEM) was conducted to characterize the particle size and shape. The particles were prepared by treating the stock suspensions in an ultrasonic bath for 15 min at 42 W/L. The suspensions were diluted to a concentration of 10 µg/mL with water (HiPerSolv CHROMANORM® for HPLC). 2 µL were transferred to single slot grids, dried overnight and imaged in a Philips CM 12 Transmissions Electron Microscope at 80 kV. For the determination of NP and MP size, 100 particles each were measured.

2.3. Characterization of PS-nano and PS-micro and detection of particle translocation by asymmetrical flow field-flow fractionation (AF4)

2.3.1. Applied fractionation system

The samples were separated and analysed using an asymmetrical flow field-flow fractionation system (AF4) (AF2000, Postnova Analytics GmbH, Landsberg am Lech, Germany). The system was equipped with an autosampler (PN5300), channel thermostat (PN4020), UV (PN3211) and Multi-Angle Light Scattering MALS (PN3621, 21 angles) detectors as well as a Smart Stream Splitter (PN1650). A channel with a tip to tip length of 277 mm, a Mylar spacer with a thickness of 350 µm and a regenerated cellulose membrane with a cut-off of 100 kDa was used for all measurements. The UV detection was conducted at a wavelength of 254 nm, and the MALS detector provided the gyration radius (calculated using the sphere model). The thermostat was set to 25 °C to stabilize the channel temperature. The autosampler temperature was kept constant at 10 °C. The data acquisition and MALS calculations were performed within the AF2000 Control Unit software (Postnova Analytics GmbH, Landsberg am Lech, Germany). The radius of gyration was evaluated with 17 active angles (20° to 148°). Spherical geometrical diameters (D_{geo}) were calculated from the diameter of gyration (D_g) based on the following relationship

$$\frac{D_g}{D_{geo}} = \sqrt{\frac{3}{5}}$$

The MALS angles were normalized with respect to the 90° angle based on a scattering form factor for spheres using a fractionation measurement of a 60 nm PS-nano size standard.

2.3.2. Applied carrier solution

Ultrapure water (UPW) was prepared using a Milli-Q integral 5 Millipore system (EMD Merck Millipore, MA, USA), with subsequent vacuum filtration through a 0.1 µm pore membrane (Durapore, Merck Millipore, Ireland). The NovaChem (NC) 100 surfactant (Postnova Analytics GmbH, Landsberg am Lech, Germany) was filtered through a 0.22 µm hydrophilic PVDF syringe filter (Millex, Merck Millipore, Darmstadt, Germany) before usage. The applied AF4-carrier liquid consisted of 0.05% (*v*/v) filtered NC in UPW.

2.3.3. Applied fractionation methods

The focusing step was performed with an injection flow of 0.2 mL min^{-1} and 7 min injection time. The elution profile for the PS-nano consisted of a 7 min constant cross flow at 1 mL min^{-1}, followed by 40 min of an exponentially decreasing cross flow, continuing with 15 min cross flow of 0.1 mL min^{-1}. A rinse step of 22 min was applied to check potential particle release and to ensure reproducible measurements.

For the PS-micro an initial cross flow of 0.5 mL min^{-1} was kept constant for 7 min. The cross flow was then decreased to 0.1 mL min^{-1} in 30 min by an exponential decay and kept constant at 0.1 mL min^{-1} for another 20 min. Afterwards, a rinse step of 17 min was applied to flush the system.

Above described methods were applied for both characterizing the native PS-particle suspensions in the different cell culture media as well as the samples obtained from the translocation studies. However, while for the characterization of the PS-particles in native suspensions and cell culture media, UV- and MALS-detection was used in order to determine respective PS-particle sizes, only UV-detection was used to prove the presence or absence of PS-particles in the translocation samples.

The basolateral samples from the translocation studies were measured as received; the apical samples were diluted with UPW up to a factor of 30 to have a sufficient injection volume and concentration for AF4-UV-MALS measurements.

2.3.4. Determination of the limit of detection and limit of quantification of the AF4 system

Limit of detection (LOD) and quantification (LOQ) were determined for AF4-UV-measurements based on the three and ten sigma (3σ and 10σ) criterion respectively. Therefore, the sensitivity of the UV signal towards the PS particles was evaluated with duplicate measurements of three different concentrations. The noise for both particle-media suspensions was calculated from at least three blank measurements by determining the standard deviation of the noise. For all measurements, 60% of the detector flow was split in order to enhance the sensitivity of the AF4-UV-MALS system.

2.4. ζ-potential measurements

For zeta potential measurements, 10 µL of the particle stock solution were added to 990 µL of cell culture medium and transferred to folded capillary cells (DTS1070, Malvern Panalytical, Malvern, United Kingdom). Electrophoretic mobility was measured by laser Doppler Micro-electrophoresis at 25 °C, three times with 10 to 100 runs (Zetasizer NanoZS, Malvern Panalytical, Malvern, United Kingdom) and the zeta potential was calculated by Zetasizer NanoZS software.

2.5. Cell culture

Caco-2, a human adenocarcinoma cell line with epithelial morphology, was obtained from DSMZ (Deutsche Sammlung für Mikroorganismen und Zellkulturen GmbH, Braunschweig, Germany). HT29-MTX-E12, a mucus-secreting subclone from colon adenocarcinoma HT29 cells, differentiated into mature goblet cells by methotrexate, was obtained from Sigma-Aldrich (Germany). Both cell lines were cultured in DMEM high glucose (4.5 g/L) (Invitrogen, Germany) supplemented with 10% FCS (Invitrogen, Germany), 2 mM L-Glutamine (Invitrogen, Germany), 1% penicillin/streptomycin (Invitrogen, Germany), 1% non-essential amino acids (Invitrogen, Germany). HPEC-A2 cells (SV40-transformed microvascular human placental venous endothelial cells) and the human placental choriocarcinoma cell line BeWo b30 were cultured in endothelial medium (EM; endothelial cell growth medium MV supplemented with one vial Supplement Mix according to the manufacturer's guide (PromoCell, Heidelberg, Germany) and 1% penicillin/streptomycin or trophoblast medium (TM; Ham's F-12 K medium supplemented with 10% FCS, 1% penicillin/streptomycin and 2 mM L-Glutamine, respectively (Aengenheister et al., 2018). NIH/3 T3, a murine fibroblast cell line, was obtained from ATCC (American Type Culture Collection, USA) and maintained using DMEM high glucose (4.5 g/L) medium supplemented with 2 mM L-glutamine, FCS (17% *v*/v), 2 mM non-essential amino acids, streptomycin (100 mg/mL) and penicillin G (100 U/mL). mES-D3, a murine embryonic stem cell line, was obtained from ATCC (American Type Culture Collection, USA) and maintained using DMEM high glucose (4.5 g/L) medium supplemented with 2 mM L-glutamine, FCS (10% v/v), streptomycin (100 mg/mL) and penicillin G (100 U/mL). HepG2CDKN1A-DsRed, a p53-sensitive reporter cell line based on the human liver carcinoma cell line, was obtained from the lab of Metka Filipic (Blagus et al., 2014) and maintained using MEM medium supplemented with 2 mM L-glutamine, heat-inactivated FCS (10% v/v), 1% non-essential amino acids, streptomycin (100 mg/mL) and penicillin G (100 U/mL). CHO-K1 cells were obtained from DSMZ (Braunschweig, Germany) and cultured in 90% Ham's F12 containing 10% heat-inactivated FBS, streptomycin (100 mg/mL) and penicillin G (100 U/mL). All cell lines were cultivated in a humidified incubator at 37 °C with 5% CO_2 atmosphere and were passaged twice a week.

2.6. Cell viability assays

For the determination of the viability of the GIT co-culture model, Caco-2 and HT29-MTX-E12 cells were seeded in a ratio of 90:10 (1×10^4 cells per well; three replicates were done per condition and experiment) on Transwell® inserts (pore size of 3.0 µm, growth area of 1.12 cm^2, Corning, USA). On day 21 of Caco-2/HT29-MTX-E12-culture, the particles were applied to the cells in a concentration range from 0.1 to 100 µg/mL for 24 h. Afterwards cell viability was determined *via* WST-1 cell proliferation reagent (Roche, Germany) according to the manufacturer's operating instruction. The absorption was determined at 450 nm (reference wavelength 690 nm), and the values were blank-corrected. Viability of the control (cells exposed to particle-free medium) was set to 100%.

The influence of the PS particles on BeWo cell viability was assessed using the MTS assay. Cells were seeded in a 96-well plate (1×10^4 cells per well; three replicates were done per condition and experiment) for 24 h and subsequently treated with different concentrations of the PS particles. As negative control, cells without treatment were used. After incubation (24 h) at 37 °C and 5% CO_2, the MTS assay (CellTiter96® AQueous One Solution Cell Proliferation Assay, Promega, Dübendorf, Switzerland) was performed according to the manufacturer's instructions. Optical density was measured at 490 nm with a microplate reader (Mithras2 LB 943, Berthold Technologies GmbH, Zug, Switzerland). OD values were blank-corrected and normalized to untreated controls. Potential interference of the PS particles with the MTS assay was excluded beforehand.

To assess PS particle toxicity on mES-D3 and NIH/3 T3 cells in 2D, cell suspensions of NIH/3 T3 and mES-D3-cells were prepared in growth media (1×10^4 cells/mL) and were transferred to 0.1% gelatin-coated 96-well cell culture plates (50 µL/well). All peripheral wells of the assay plate were filled with 200 µL growth media. A 7-point serial dilution in growth media was prepared for each test compound and was transferred to the assay plate 2 h after cell seeding (150 µL/well). Afterwards, the cells were incubated in humidified atmosphere at 37 °C and 5% CO_2. Three and five days after seeding the cell supernatant was replaced by freshly prepared PS particle solution (200 µL/well). Seven days after seeding the assay plate was taken out of the incubator and located at room temperature for 10 min, before cell supernatant was aspirated (80 µL/well) and CellTiter-Glo reagent (Promega, Inc.) were dispensed (50 µL/well). Afterwards, the assay plate was placed on a shaker for 1 min. After 10 min incubation at room temperature, the luminescence signal was detected on an EnVision plate reader (PerkinElmer Inc.).

2.7. Mouse ES-D3 differentiation assay in hanging drop

The mES-D3 differentiation assay was performed according to Seiler and Spielmann, 2011. A 7-point dilution series was prepared in growth media for each PS particle type. A suspension of mES-D3 cells (3.75 x 10^4 cells/mL) was mixed with the compound solution. 20 µL drops of cell suspension (750 cells/drop) with PS particles were placed on the underside of a 100 mm tissue culture Petri dish lid, at minimum 40 drops per lid. Separate Petri dishes were used for each concentration of test compound, untreated control, and solvent control. The Petri dish was filled with 5 mL PBS and the lid was carefully turned and put on top. After three days of incubation at 37 °C and 5% CO_2 in humidified atmosphere the embryoid bodies (EB) were rinsed from the lid with 5 mL of freshly prepared compound solution into a 60 mm Ø Petri dish. The EB suspension was incubated for two days. On day 5 of the assay, a fresh compound dilution series was prepared in media and transferred into 24-well cell culture plates (1 mL/well). A separate 24-well plate was used for each compound concentration, untreated control and solvent control (24 wells per condition). One EB was transferred from the Petri dish into each well of the 24-well plate. After further 5 days of incubation (= day ten of the assay), cardiomyocyte contraction was determined in each well under the light microscope by optical inspection. Evaluation of the results was based upon 3 endpoints determined in two cell lines: ID_{50}, reflecting 50% inhibition of mES-D3cell differentiation, IC_{50} mES-D3, reflecting 50% inhibition of mES-D3 cell growth, and IC_{50} 3 T3, indicating 50% inhibition of NIH 3 T3 cell growth.

To predict embryotoxic potential, the prediction model (PM) originally proposed by Seiler and Spielmann, 2011 for the EST was refined using data obtained during a prevalidation study. Basically, for the improved prediction model (iPM), the endpoints were not changed, except that IC_{50} and ID_{50} concentrations above 1000 µg/mL are not calculated. If IC_{50} or DC_{50} value exceeds this concentration, it is set to 1000 µg/mL by definition, which implies that for future testing, the maximum test concentration will be 1000 µg/mL. ln the iPM, the combination of endpoints, which were applied as variants in the previous linear discriminant analysis, have been modified:

Function I: 5.92*lg(IC_{50} 3 T3) + 3.5*lg(IC_{50} mESC)-5.31*(IC_{50} 3 T3-ID_{50})/IC_{50} 3 T3–15.7.
Function II: 3.65*lg(IC_{50} 3 T3) + 2.39*lg(IC_{50} mESC)-2.03*(IC_{50} 3 T3-ID_{50})/IC_{50} 3 T3–6.85.
Function III: −0.125*lg(IC_{50} 3 T3)-1.92*lg(IC_{50} mESC) + 1.5*(IC_{50} 3 T3-ID_{50})/ IC_{50} 3 T3–2.67.

The classification was based on the following criteria. Non-embryotoxic particles comply with the following rule function I > function II and function I > function III, weakly embryotoxic particles show function II > function I and function II > function III and strongly embryotoxic particles comply to the rule function III > function I and function III > function II.

2.8. In vitro translocation studies

For transport studies of the particles through the biological barriers, cells were seeded on polycarbonate Transwell® inserts (pore size 3.0 µm, growth area 1.12 cm^2, apical volume 0.5 mL, basolateral volume 1.5 mL; Corning®, Sigma-Aldrich, Buchs, Switzerland). Caco-2 and HT29-MTX-E12 cells were seeded in a ratio of 90:10 at a density of 1.0×10^5 cells per well on inserts and cultured for 21 days with medium exchange every second day. BeWo b30/HPEC-A2 co-cultures were performed as described previously (Aengenheister et al., 2018). Briefly, inserts were pre-coated with 50 µg/mL human placental collagen IV (Sigma-Aldrich, Buchs, Switzerland) for 1 h at 37 °C/ 5% CO_2. For the co-culture, firstly HPECs were cultivated on the basolateral side for 2 h followed by seeding the BeWo cells on the apical side. The cells were cultivated for 3 days with medium exchange every second day.

To determine the translocation *in vitro*, fresh medium was given to the basolateral chambers, and 10 µg/mL or 100 µg/mL of PS particles were applied apically. Then cells were incubated for 24 h under static conditions. The transepithelial electrical resistance (TEER) of the intestinal co-culture was continuously measured during the exposure duration (24 h) *via* cellZscope® device (nanoAnalytics, Germany). Before and after PS exposure, the TEER of the placental co-culture was measured with a chopstick electrode (STX3, World Precision Instruments Inc., Sarasota, USA). TEER values for the cell layer were obtained by subtracting the intrinsic resistance (blank insert membrane) from the total resistance (insert membrane with cells) and were corrected for the surface area (Ω cm^2). At the end of the exposure, apical and basolateral samples were collected for AF4 measurements to determine particle translocation. Samples were also taken from the applied PS working suspension and blank cell culture medium of each experiment as controls for the AF4 measurements. Membranes with intestinal and placental cells were fixed in 4% paraformaldehyde (Sigma-Aldrich, Buchs, Switzerland) for 15 min at room temperature (RT), washed two times in phosphate buffered saline (PBS) and stored in 30% sucrose (Sigma-Aldrich, Steinheim, Germany) at 4 °C for further immunocytochemistry staining.

2.9. Immunocytochemistry (ICC)

For ICC staining fixed cells on inserts were washed with PBS and further incubated in 0.1% Triton X-100 (Sigma-Aldrich, Buchs, Switzerland) for 15 min at RT. After washing with PBS, membranes were incubated for 30 min in 5% BSA at RT. Then, for the actin staining, the phalloidin Alexa Fluor 647 (Thermo Fisher Scientific, Germany) or phalloidin Alexa Fluor 633 (Invitrogen, Frederick, MD, USA) were diluted 1:50 in 0.5% BSA in PBS and applied on the intestinal and placental cells for 60 min at RT, respectively. 40,6-diamidine-2-phenylindole (DAPI; Sigma-Aldrich, Buchs, Switzerland; 10 min at RT, 1:1000) was included during one PBS washing step. To obtain flat membranes, whole inserts were embedded with NeoMount (Merck, Darmstadt, Germany) or Mowiol 4–88 (Sigma-Aldrich, Buchs, Switzerland) and membranes were cut off from the holder with a scalpel after drying of the embedding medium. Images and z-stacks were acquired with confocal laser scanning microscopes (CLSM TCS SP8, Leica, Nussloch, Germany and CLSM 780, Zeiss, Feldbach, Switzerland).

2.10. p53 reporter gene assay

The assay was performed using black, clear-bottom, 348-well plates (PerkinElmer Inc., Waltham, USA). HepG2CDKN1A-DsRed biosensor cells were seeded at a density of 2000 cells per well in a volume of 25 µL. The cells were incubated at 37 °C in 5% CO_2 and placed in an IncuCyte ZOOM (Essen BioScience Ltd., Welwyn Garden City, United Kingdom). DsRed fluorescence was determined every two hours for up to 48 h and analysed by measuring the area under the curve using GraphPad Prism version 7.00 for Windows (GraphPad Software, La Jolla, USA).

2.11. Micronucleus assay

The assay was performed using black, clear-bottom, 348-well plates (PerkinElmer Inc., Waltham, USA). CHO-K1 cells were seeded at a density of 500 cells per well in 20 µL and incubated at 37 °C in 5% CO_2 for 2 h prior PS particle addition. PS particle addition was performed by adding 5 µL of growth medium including appropriate particle concentration to each well. Growth medium was exchanged after 24 h with medium containing 3 µg/mL Cytochalasin B. After 18 h medium was exchanged again, using normal growth medium. Cells were fixed after one to two h of incubation in normal medium using 3.8% PFA in PBS for 20 min. Afterwards the cells were permeabilized using 0.3% TritonX-100 in PBS for 5 min and stained using 800 nM Hoechst 33258 in TBS-T. Image acquisition was performed on an Opera microscope (PerkinElmer Inc., USA) and analysed using Columbus 2.7.1.133403 (PerkinElmer Inc., USA).

2.12. Statistical analysis for all biological assays performed in this study

Results were generated from three independent experiments ($n = 3$) with a minimum of three technical replicates unless stated otherwise. The data is presented as mean with standard deviation (SD). Effects were compared to non-treated cells. Statistical analysis was done by one-way ANOVA. A values are marked by * as $p < .05$, ** as $p < .01$ and as *** as $p < .001$.

3. Results

In contrast to single-organ studies, this multi-endpoint study provides a consistent data set to assess the toxic potential and compare organ-specific outcomes of PS nano- and microparticles, used as representatives for NP and MP, *in vitro*.

3.1. Characterization of the PS-nano and PS-micro

In this study, negatively charged PS nanoparticles and microparticles were characterized by different methods. TEM images of the particles in water (Fig. 1) confirm their spherical shape and diameter measurements resulted in 46.3 ± 6 nm for PS nanoparticles (PS-nano, $n = 100$) and 465.8 ± 10.2 nm for PS microparticles (PS-micro, n = 100), respectively. The diameter of gyration (D_g) and geometrical spherical diameter (D_{geo}) were determined in the different cell culture media (CCM) by AF4-UV-MALS (Table 1). The size characteristics in the different CCM are comparable to the size determined by TEM images. The zeta potential of the PS particles was measured in all serum containing CCM used in this study (DMEM, EM, and RPMI). The surface charge of PS particles in CCM was always negative between −11.4 mV ± 1.4 mV to −12.0 mV ± 0.7 mV for PS-nano and − 8.8 mV ± 0.3 mV to −11.6 mV ± 0.5 mV for PS-micro. The

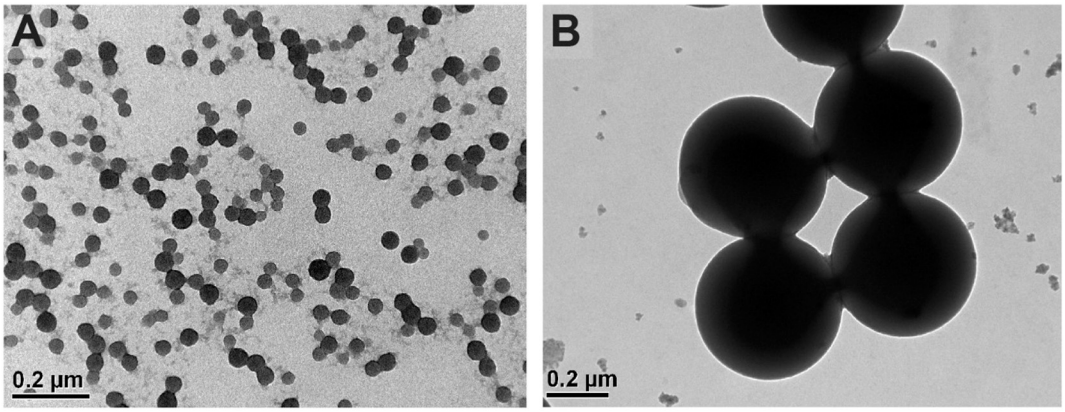

Fig. 1. TEM image of the negatively charged 50 nm PS-nano (A) and 0.5 µm PS-micro (B) in water.

Table 1
Physicochemical characterization of PS-nano and PS-micro. The diameter was determined *via* AF4-UV-MALS, D_g = Diameter of gyration determined at the UV-peak maximum, D_{geo} = geometrical diameter. Surface charge of the particles is presented as ζ-potential. Data represent the mean ± SD of three independent measurements.

		D_g (nm)	D_{geo} (nm)	ζ-potential (mV)
Solvent				
PS-nano	Ultrapure water	36 ± 1	47 ± 1	-58.2 ± 1.1
PS-micro	Ultrapure water	447 ± 3	577 ± 4	−36.1 ± 0.4
Cell culture medium				
PS-nano	DMEM + 10 % FCS	49 ± 2	64 ± 2	-11.6 ± 0.6
	DMEM +17% FCS	45 ± 2	58 ± 2	−9.0 ± 0.5
	RPMI +10% FCS	44 ± 2	57 ± 2	−12.0 ± 0.7
	Ham's F12 + 10% FCS	46 ± 2	59 ± 2	−10.0 ± 0.5
	EM + 5% FCS	40 ± 2	51 ± 2	−11.4 ± 1.4
PS-micro	DMEM +10% FCS	438 ± 4	565 ± 4	−9.2 ± 0.3
	DMEM +17% FCS	451 ± 6	582 ± 6	−9.1 ± 0.8
	RPMI +10% FCS	447 ± 2	577 ± 2	−11.6 ± 0.5
	EM + 5% FCS	436 ± 4	563 ± 4	−8.8 ± 0.3
	Ham's F12 + 10% FCS	463 ± 4	597 ± 5	−9.9 ± 1.0

surface coverage with carboxylic groups was determined to be 70 ± 10 µmol/g COOH for PS-nano and 105 ± 10 µmol/g COOH for PS-micro.

3.2. Toxicology studies in human GIT and placenta barrier models

3.2.1. Cell viability

The cell viability of the intestinal co-culture (Caco-2/HT29-MTX-E12) and placental trophoblast cells (BeWo b30) were determined for PS-nano and PS-micro in different concentrations (0.01 - 100 µg/mL) by WST-1 and MTS assay, respectively. PS-nano did not affect the viability of intestinal cells up to 50 µg/mL but caused a significant ($p \leq .05$) increase in metabolic activity at 100 µg/mL (Fig. 2A). PS-micro induced a decrease in metabolic activity only at a concentration of 0.01 µg/mL (Fig. 2B). In the placental cell model, PS-nano induced a slight but significant ($p \leq .05$) increase in metabolic activity at concentrations higher than 5 µg/mL (Fig. 2C). PS-micro increased mitochondrial activity only at concentrations from 0.01–10 µg/mL (Fig. 2D).

3.2.2. Barrier integrity

For determining the impact of the PS particles on intestinal and placental barrier integrity, the trans-epithelial electrical resistance (TEER) was measured before and after the exposure to 10 µg/mL and 100 µg/mL PS-nano and PS-micro for 24 h, respectively. The tightness of the intestinal co-culture was not affected by PS-nano and PS-micro at both concentrations (Fig. 3A). Similarly, the placental co-culture exposed to PS-nano and PS-micro did not show any significant decreases in TEER values after the treatment with particles (Fig. 3B).

3.3. Translocation across biological barriers

Translocation of PS-nano and PS-micro across the intestinal and placental barrier was determined by asymmetrical flow field-flow fractionation (AF4). The limit of detection (LOD) and limit of quantification (LOQ) for PS-nano and PS-micro in the different media are summarized in Table S1.

Pre-studies verified the transport of the particles across control Transwell® membranes without cells (Fig. S1). After 24 h of exposure to 10 and 100 µg/mL, PS-nano and PS-micro were detected in the apical but not in the basolateral compartment of intestinal and placental co-cultures by AF4-UV analysis (Figs. 4 and 5).

3.4. Cellular uptake and intracellular distribution

To investigate particle uptake and intracellular distribution qualitatively, intestinal and placental co-cultures exposed to particles for 24 h were stained for nuclei and actin filaments and characterized by confocal laser scanning microscopy (CLSM). In contrast to untreated controls (Fig. 6A and D), PS-nano and PS-micro were internalized by intestinal and placental cells (Fig. 6B-F). For the placental co-cultures, uptake was only apparent in the BeWo b30 trophoblast cells on the apical side of the insert but not in HPEC-A2 endothelial cells cultivated on the basolateral side (Fig 6E2 and F2). Particles were not homogenously distributed in the cell layers but were found in single spots of the samples.

3.5. Embryotoxicity

To understand the embryotoxic potential of PS-nano and PS-micro, the embryonic stem cell (ESC) assay was performed. The ESC test assesses three endpoints: cytotoxic effects on NIH/3 T3 fibroblasts and mouse embryonic stem cells (mES-D3) as well as the inhibition of the differentiation into beating cardiomyocytes (Seiler and Spielmann, 2011). Embryotoxicity is identified as a relation of the corresponding IC_{50} and ID_{50} values. The IC_{50} value of PS-nano for NIH/3 T3 fibroblasts and mES-3D could not be determined because they were not toxic in the tested concentration range (0.01–100 µg/mL) (Fig. 7A and B). For PS-micro, the IC_{50} was 12.6 µg/mL for NIH/3 T3 cells and mES-3D (Fig. 7 A, B and D). In the case of mES cells, the IC_{50} for PS-nano was higher than 100 µg/mL and therefore not identified in the tested concentration range. The differentiation into beating cardiomyocytes was inhibited at a dose of 89.9 µg/mL PS-nano and 0.1 µg/mL PS-micro (ID_{50}) (Fig. 7 C and D). Overall, the classification calculated according to Seiler and Spielmann resulted in weak embryotoxicity of the investigated PS-nano

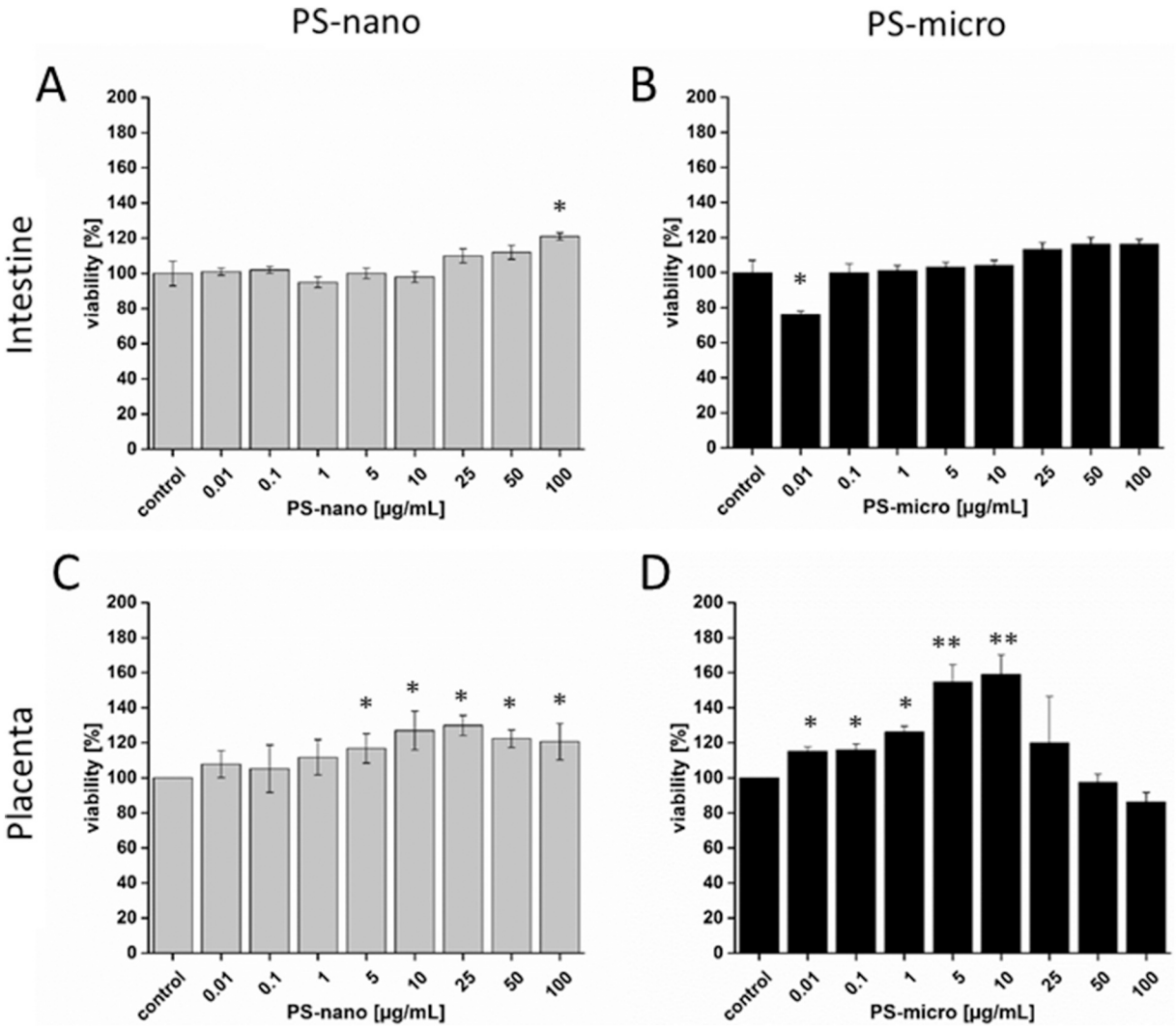

Fig. 2. Cell viability of intestinal co-cultures and placental trophoblasts after exposure to PS-nano and PS-micro. Caco-2/HT29-MTX-E12 co-cultures (A + B) and BeWo b30 cells (C + D) were treated with PS-nano (A + C) or PS-micro (B + D) in a concentration range of 0.01 µg/mL to 100 µg/mL for 24 h. Data represent the mean ± SD of three independent measurements; $^{*}p \leq .05$ compared to untreated cells, $^{**}p \leq .01$ compared to untreated cells.

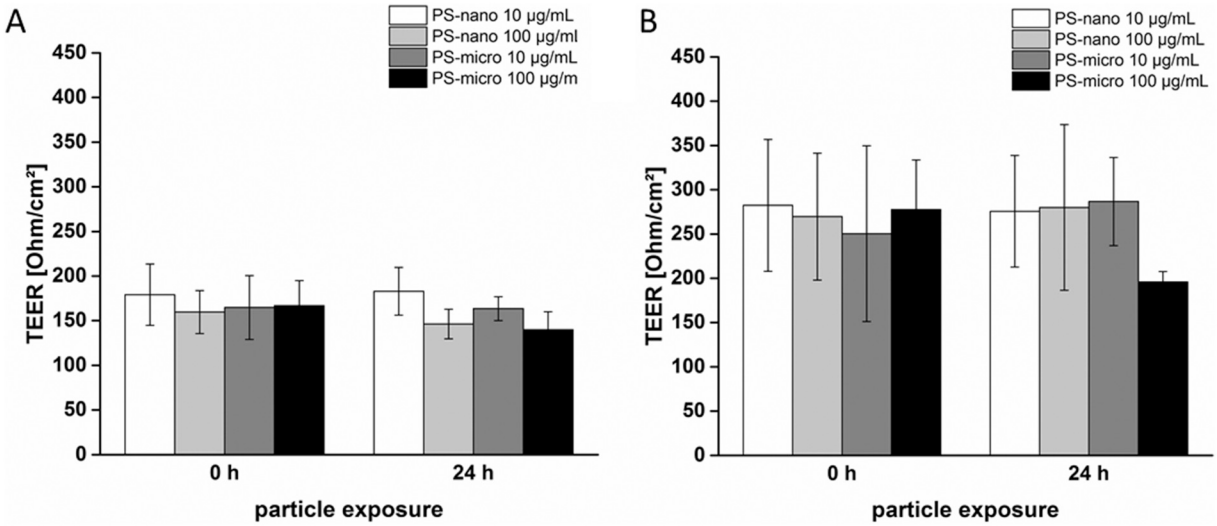

Fig. 3. Impact of PS-nano and PS-micro on barrier integrity of the *in vitro* GIT- and placental barrier model, (A): TEER values of the intestinal co-culture before (0 h) and after exposure (24 h) to 10 and 100 µg/mL of PS-nano or PS–micro (dark grey and black). B: TEER values of the placental co-culture before (0 h) and after exposure (24 h) to 10 and 100 µg/mL PS-nano or PS–micro. Data represent the mean ± SD of three independent measurements.

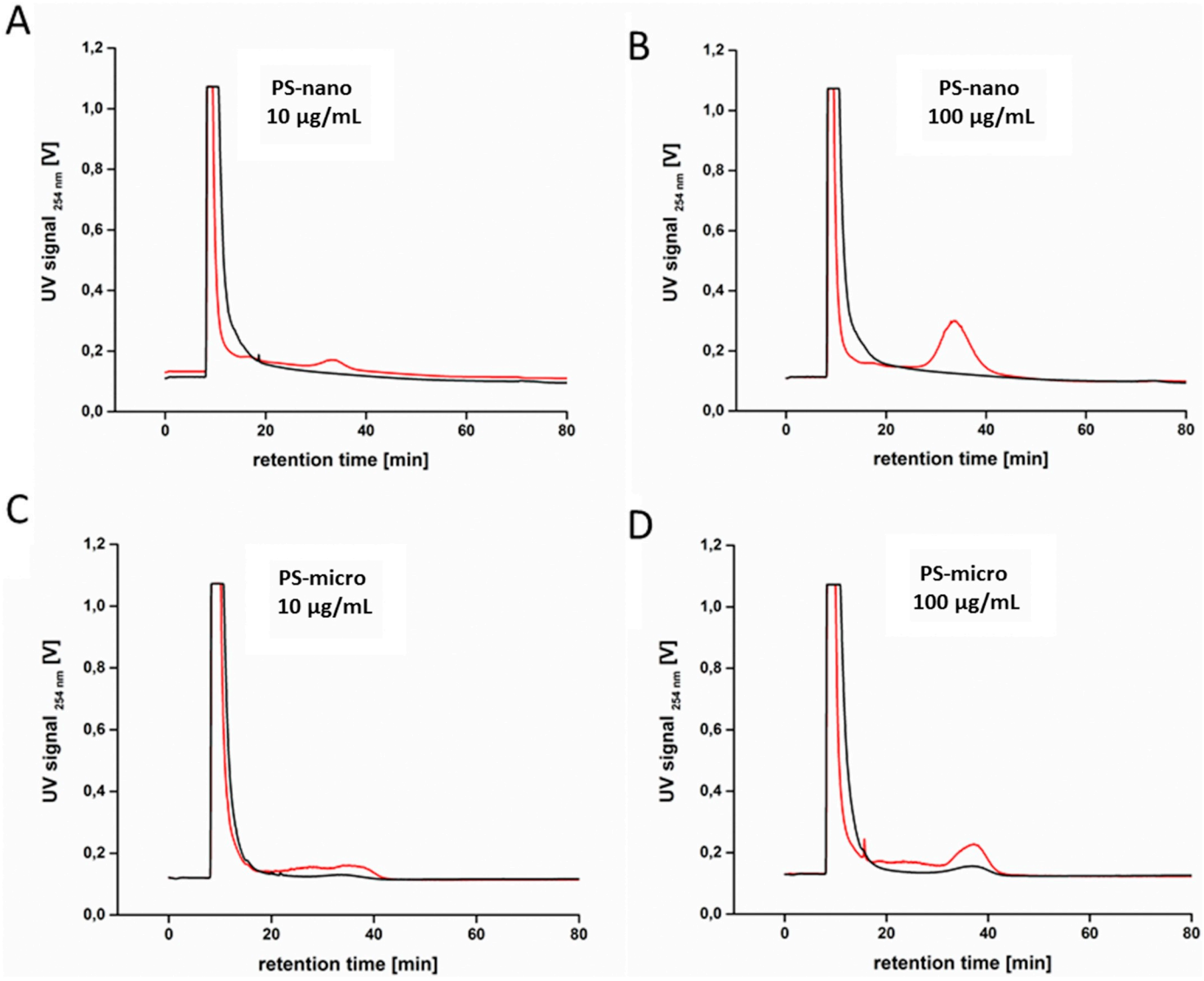

Fig. 4. Translocation of PS-nano and PS–micro across the intestinal barrier *in vitro*. Co-cultures were exposed to 10 or 100 µg/mL of PS-nano (A + B) and PS-micro (C + D) for 24 h. Particles were detected in apical (red line) and basolateral (black line) supernatants by AF4-UV at a retention time of 30 min. Concentrations of PS-nano and PS-micro in the basolateral compartments were below the LOD of AF4-UV (69 µg/L PS-nano, 12 µg/L PS–micro) for all investigated concentrations and sizes. Graphs are representative for three independent experiments and runs. (For interpretation of the references to colour in this figure legend, the reader is referred to the web version of this article.)

and -micro (Fig. 7 D) (Seiler and Spielmann, 2011). This classification is a result of the slightly higher effect on differentiation (lower ID_{50}) compared to the toxicity of the tested material.

3.6. Genotoxicity

As genotoxicity is a critical factor in our toxicity assessment, we used two different assays to analyse different pathways. The p53 reporter gene assay was performed to check for p53 activation, as it is based on the promotor of a major downstream target of activated p53, CDKN1A, which drives the expression of DsRed2 in this biosensor. Alternatively, we also checked for particle-induced DNA double-strand breaks by a micronucleus assay.

3.6.1. p53 expression

For the detection of possible genotoxic effects of PS-nano and -micro, cells were imaged every two hours for 48 h, and fluorescence intensity was integrated. At higher concentrations (> 100 µg/mL for PS-nano and > 25 µg/mL for PS-micro), the particles interfered with the assay due to their fluorescent labelling, and therefore they were excluded from the analysis. The expression level induced by colchicine was used to identify a genotoxic compound or particle and served as positive control. As neither PS-nano nor PS-micro did reach this activation level, these particles were non-genotoxic at the indicated concentration (Fig. 8A and B).

3.6.2. Micronuclei formation

In addition, genotoxicity was analysed using a protocol adapted from the OECD protocol 487 (Aardema et al., 2006). This micronucleus assay is ideally suited to identify aneugens and clastogens and was validated at different laboratories, resulting in a high degree of confidence in the generated data. No genotoxicity was observed in the micronucleus assay (Fig. 9, Fig. S2), which is in line with the data generated using the reporter gene assay.

4. Discussion

Burns and Boxall (2018) conclude in their review that one missing

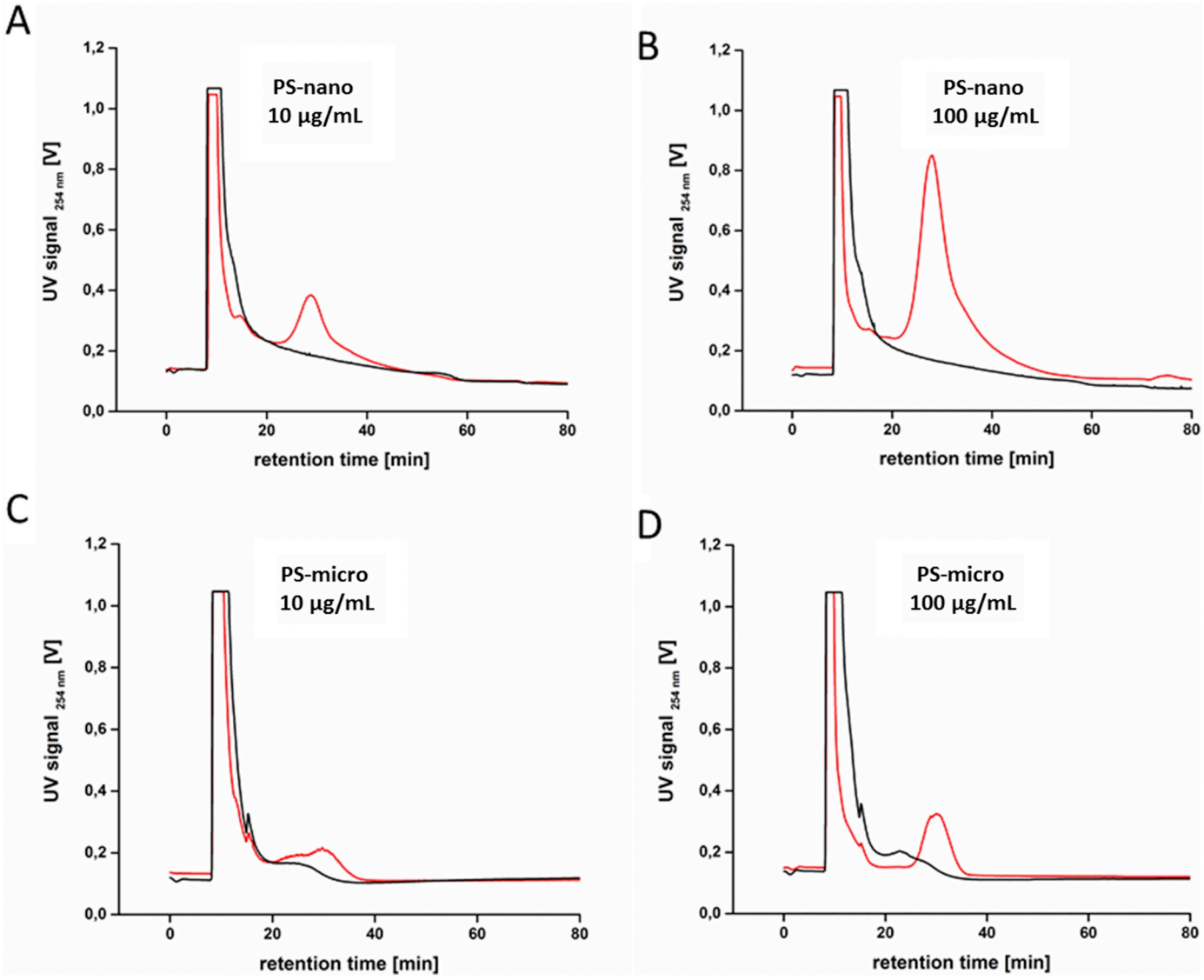

Fig. 5. Translocation of PS-nano and PS–micro across the placental barrier *in vitro*. Co-cultures were exposed to 10 or 100 µg/mL of PS-nano (A + B) and PS-micro (C + D) for 24 h and particles were detected in apical (red line) and basolateral (black line) supernatants by AF4-UV at a retention time of 30 min. Concentrations of PS-nano and PS-micro in the basolateral compartments were below the LOD of AF4-UV (82 µg/L PS-nano, 86 µg/L PS–micro) for all investigated concentrations and sizes. Graphs are representative for three independent experiments and runs. (For interpretation of the references to colour in this figure legend, the reader is referred to the web version of this article.)

aspect in the field of NP and MP research is their effect characterization. Effect studies are needed on the types of MP that occur in the environment and on their transformation products, such as NP (Burns and Boxall, 2018). Our study tries to address this knowledge gap by evaluating the impact of PS-nano and PS-micro on different key endpoints of acute toxicity *in vitro*, including assays relevant to highly sensitive populations such as the developing embryo (*i.e.*, placental transfer and embryonic stem cell assay).

PS particles with sizes of 0.5 µm and 50 nm were used as representatives for MP and NP, respectively. The primary size of the particles obtained from TEM measurements did not change in the different media as confirmed by AF4-UV-MALS analysis indicating that different media compositions and supplements did not have a strong influence on particle agglomeration. Besides size, surface charge and functionalization with ligands can play a decisive role in the uptake mechanisms and toxicity profile of particles (Chiu et al., 2015; Fischer et al., 2003; Tenzer et al., 2013). For instance, Asati et al., 2011 described that positively charged and neutral cerium oxide nanoparticles were preferentially taken up by human cells in comparison to negatively charged particles and were recovered in different cell compartments depending on their surface charge (Asati et al., 2010, 2011). Similarly, the pulmonary toxicity of stearylamine-polylactic acid (PLA) polymers in mice was higher for positively than negatively charged particles, due to enhanced cellular uptake and localisation of cationic particles in the lung (Harush-Frenkel et al., 2010). The PS particles used in this study were functionalized with carboxyl groups (COOH). The surface charge of PS-nano and PS-micro were similar and slightly negative in the different media, which can be explained by the fact that proteins (mainly the BSA) contained in the fetal calf serum are forming a protein corona around the particles dominating the overall charge of the particles (Kloet et al., 2015). Nevertheless, differences may exist in the density or type of protein coating between PS-nano and –micro, which could affect particle adhesion, uptake and subsequent biological responses by the cells.

The mass production of MP and the breakdown products of meso-scaled plastic inevitably results in an increase of MP release into the environment with currently unknown consequences. Presently, there are no factual data, only few probabilistic material flow model data

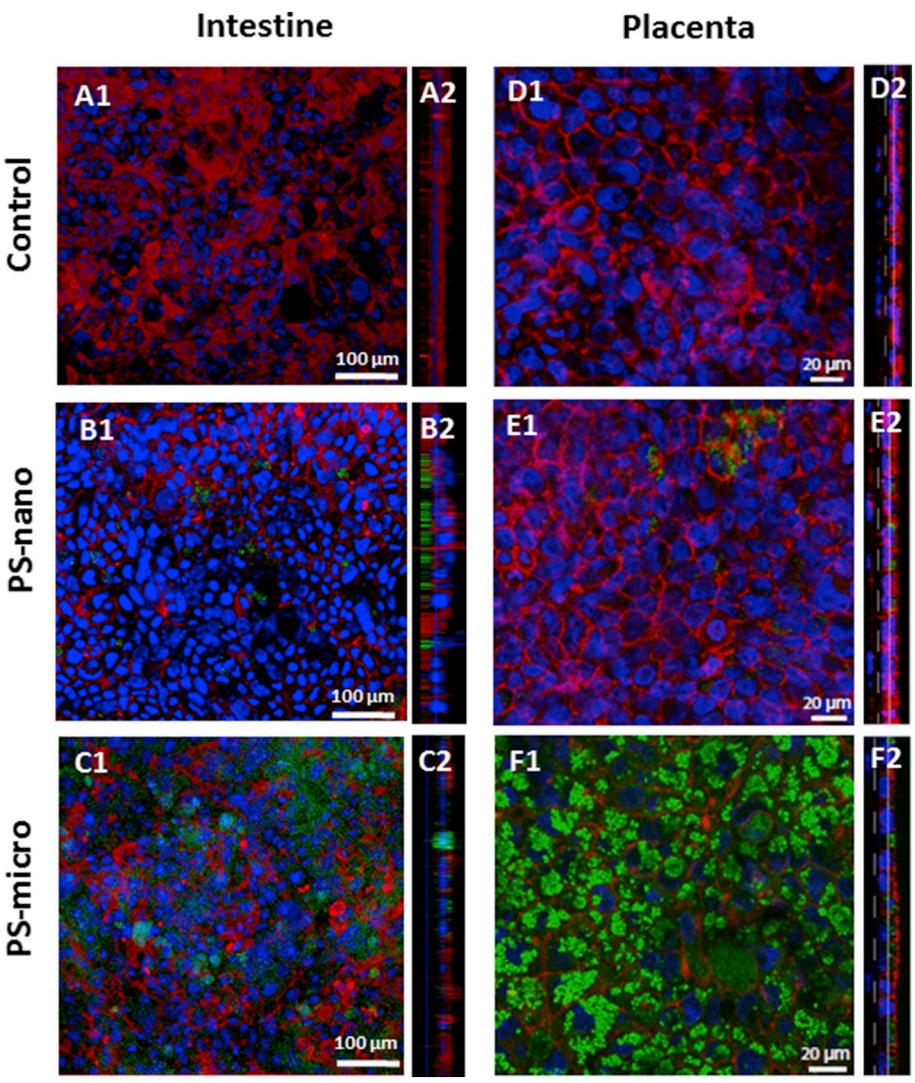

Fig. 6. Internalization of PS-nano and PS-micro by intestinal and placental co-cultures. Confocal micrographs of Caco-2/HT29-MTX-E12 (A-C) and BeWo b30/HPEC-A2 co-cultures (D-F) after 24 h of exposure to 100 µg/mL PS-nano (B + E) and PS-micro (C + F). Cells were stained with phalloidin (actin, red) and Dapi (nuclei, blue), while fluorescently labelled PS particles (Rhodamine 6G) appear in green. A2-F2 represent x-z cross-sectional views of the cell layers and A1-F1 represent the single z-plane). Presented images are representative for all investigated samples. (For interpretation of the references to colour in this figure legend, the reader is referred to the web version of this article.)

(Adam et al., 2018; Kawecki et al., 2018), on concentrations in the environment and certainly none on their physicochemical forms or distribution (Burns and Boxall, 2018). Published quantitative research on uptake and accumulation of plastics by the organisms is scarce. Therefore, we have chosen a wide range of concentrations in our study (0.01 µg/mL – 100 µg/mL) to cover potential low as well as high, worst-case exposure scenarios. The food chain is considered the main entry path for NP and MP into the human body (Fernandes et al., 2007). In order to assess whether PS-nano and PS-micro penetrate the human intestinal barrier, we performed translocation and effect studies on intestinal *in vitro* co-cultures. In case of particle transfer to the systemic circulation, we chose the placenta as a secondary organ of interest since it is highly perfused and acts as an essential barrier to protect the developing fetus. The intestinal co-cultures were largely unaffected by PS-nano and –micro regarding their metabolic activity in the tested concentration range from 0 to 100 µg/mL. The phenomenon that lower doses could be more toxic than higher doses has been previously described (Vandenberg et al., 2012) but it remains to be shown if intestinal functionality and integrity is compromised. Since we did neither observe a decrease in TEER or an increased translocation of PS-micro, it appears that intestinal barrier function was still intact. A different metabolic response was observed for placental trophoblasts. Here, a moderate increase in mitochondrial activity was induced by PS-nano at concentrations higher than 5 µg/mL and at 0.01–10 µg/mL for PS-micro. The consequences of this increased mitochondrial activity remain to be investigated, but again, we did not observe any adverse effects on barrier integrity as TEER and PS particle translocation was not affected at all concentrations. Clearly, our study shows that different cell types react differently to the exposure to PS-nano and –micro. One reason for the different responses in intestinal and placental cells might be the robustness of the tissue types and the mucus layer, which has a protective function and is present on the upper side of the intestinal cultures but absent in placental trophoblast cultures (Drasler et al., 2017; Wright and Kelly, 2017).

To understand if PS-nano and PS-micro can cross the intact intestinal and placental co-cultures, we confirmed barrier integrity by TEER measurements for all particles. Higher SD for placental *versus* intestinal co-cultures can be explained by the use of different measurement systems (manual *versus* online). Translocation of PS particles was investigated by AF4-UV analysis. No transport across intestinal or placental co-cultures was observed for PS-nano or PS–micro even at the very high concentration of 100 µg/mL, within 24 h, but we cannot exclude that a small amount of particles below the limit of detection of the AF4 method could have been translocated. Therefore, it could be possible that a chronic exposition to PS particles over prolonged time periods may lead to a transport of low quantities of particles across these biological barriers. Previous studies have revealed a size-dependent translocation for plain PS nanoparticles in the *ex vivo* placenta perfusion model (Grafmueller et al., 2015; Wick et al., 2010) and in different intestinal *in vitro* models (Schimpel et al., 2014; Walczak et al.,

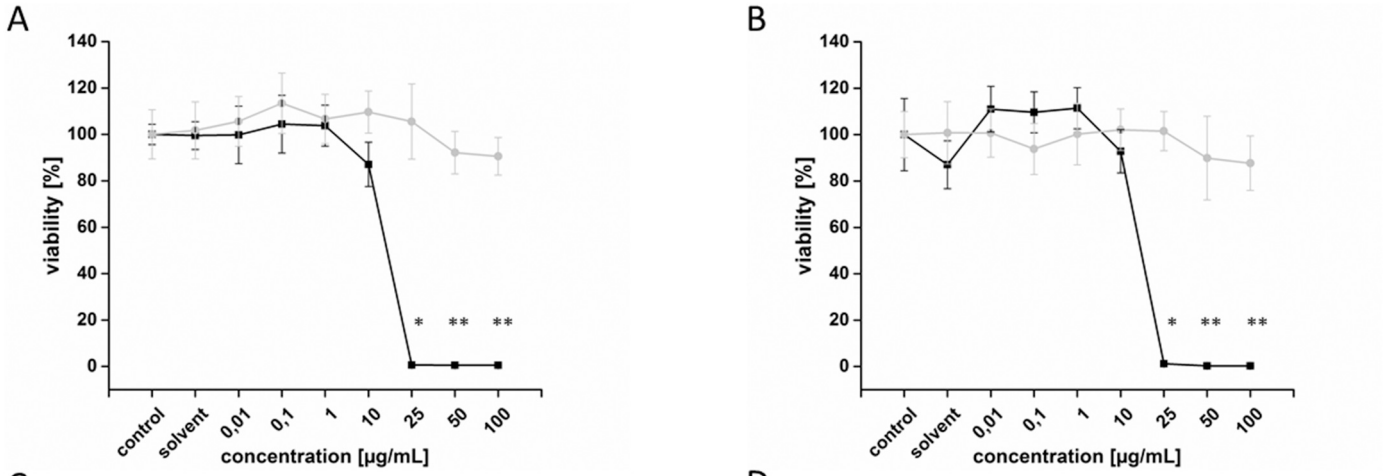

C

concentration PS-nano [µg/mL]	0	0,01	0,1	1	10	25	50	100
Wells containing EB's	24	24	24	24	24	24	24	24
Wells with myocard	24	22	23	22	23	24	23	2
Myocards %	100	91,7	95,8	91,7	95,8	100	95,8	8,3

Concentration PS-micro [µg/mL]	0	0,01	0,1	1	10	25	50	100
Wells containing EB's	24	24	24	24	24	24	24	24
Wells with myocard	24	24	20	0	0	0	0	0
Myocards %	100	100	83,3	0	0	0	0	0

D

	PS- nano	PS- micro
IC_{50} NIH/3T3	> 100 µg/mL	12.6 µg/mL
IC_{50} mESC-D3	> 100 µg/mL	12.6 µg/mL
ID_{50}	89.9 µg/mL	0.1 µg/mL
Classification	weak embryotoxic	weak embryotoxic

Fig. 7. Embryotoxicity assessment of PS-nano and PS-micro using the embryonic stem cell test (EST). (A) Toxicity in NIH/3 T3 cells. (B) Toxicity in mES-D3 cells. (C) Differentiation of cardiomyocytes. (D) Classification of the results. PS-nano is shown in light grey; PS-micro is shown in black. Data represent the mean ± SD of three independent measurements; $^{*}p \leq .05$ compared to untreated cells, $^{**}p \leq .01$ compared to untreated cells.

2015). However, consistent with our findings, the transfer was highly limited for carboxyl-modified PS nanoparticles in perfused placentas (Grafmueller et al., 2015) and in intestinal *in vitro* models where mucus-producing cells were present (Schimpel et al., 2014). Interestingly, two commercial 50 nm PS-nanoparticles with similar size and surface charge showed completely different transport behaviour across the BeWo b30 transfer model with very low resp. high permeability in a previous study (Kloet et al., 2015). In intestinal *in vitro* models, the translocation of PS nanoparticles was strongly influenced not only by size but also by the surface chemistry, where two types of negatively charged 50 nm nanoparticles showed an over 30-fold difference in translocation rate. A neutral surface charge significantly reduced the translocation rate, whereas negatively charged particles significantly increased in translocation rate (Walczak et al., 2015). The choice of the

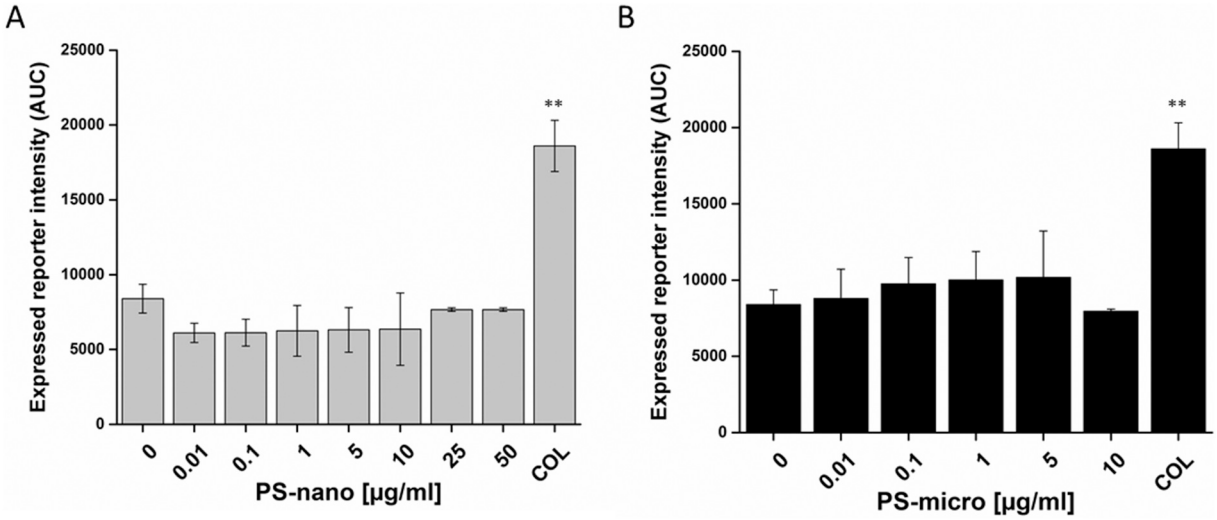

Fig. 8. Genotoxicity assessment of PS-nano and PS-micro using the p53 reporter gene assay. The area under the curve of cells exposed to different concentrations of PS-nano (A) or PS-micro (B) for 5 days. 62.5 nM colchicine was used as positive control (expression level indicated by a horizontal line). Data represent the mean ± SD of three independent measurements. $^{**}p \leq .01$ compared to untreated cells.

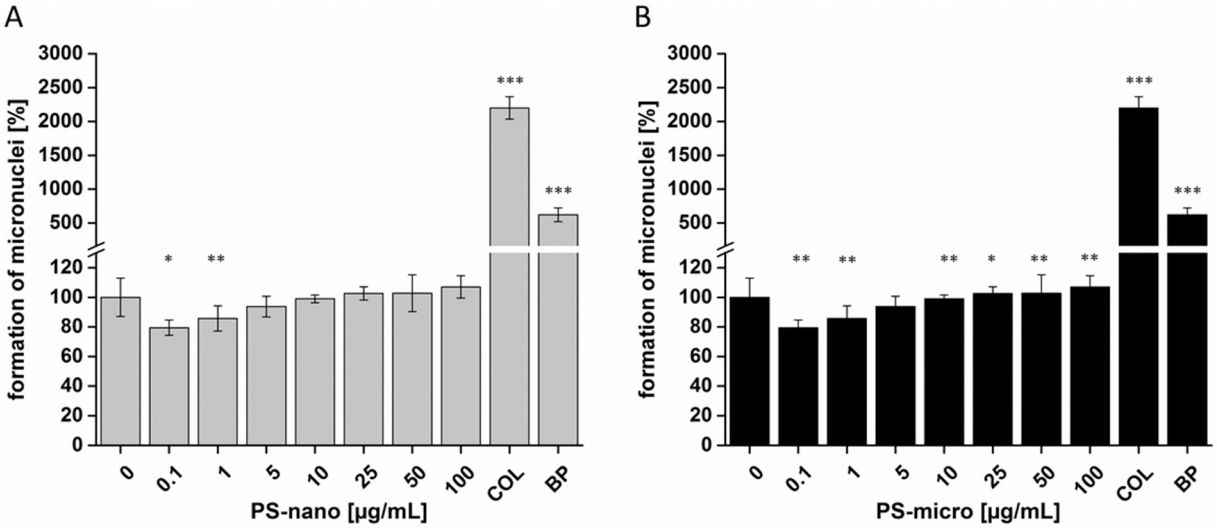

Fig. 9. Formation of micronuclei after PS-nano and PS–micro exposure. CHO-K1 cells were exposed to 0–100 µg/mL PS-nano or PS-micro before performing the micronuclei assay. 10 µM Colchicine (COL) and 10 µM Benzo[*a*]pyrene (BP) were used as positive controls. PS-nano is shown in light grey (A); PS-micro is shown in black (B). Data represent mean ± SD of three independent measurements; *p ≤ .05 compared to untreated cells, **p ≤ .01 compared to untreated cells. ***$p \leq .001$ compared to untreated cells.

intestinal *in vitro* model (mono-, co-culture or triple-culture) plays another important role, since the presence of goblet cells or M-cells can affect the translocation of particles (Walczak et al., 2015). Non-functionalized 200 nm-polystyrene particles could be shown to permeate the mucus layer and penetrate better into the epithelium, than smaller particles (Teubl et al., 2013). For these reasons, further studies using a larger variety of plastic particles with distinct properties are needed to better understand the potential placental and intestinal transfer of MP and NP.

Despite the absence of intestinal and placental translocation, confocal microscopy showed that nano- and micron-sized PS particles were internalized by intestinal and placental cells where they may accumulate and elicit potential adverse long-term effects to barrier function. This scenario would mean that particles could be released from the tissue after a certain time and distribute in another organs. A delayed release towards the systemic or fetal circulation is also conceivable. It was not possible to conclude if uptake of a specific particle was higher in intestinal *vs.* placental co-cultures since these experiments were performed in different labs with slightly different equipment and settings. Also, quantitative comparisons between PS-nano and PS–micro internalization in the same co-culture was challenging since the different particles have distinct fluorescence intensities. Higher fluorescence of larger PS-micro particles could, therefore, be misinterpreted as higher uptake and PS-nano may only be detectable if they accumulate in vesicles.

Because the PS particles were taken up by placental co-cultures and may eventually cross the barrier upon prolonged exposure as well as previously described placental transfer of another type of 50 nm COOH-PS nanoparticles (Kloet et al., 2015), we performed further investigations on the embryotoxicity of PS-nano and PS-micro. Using mice embryos at the two-cell stage Bosman et al. found no embryotoxicity using a mixture of PS nanoparticles in the size of 40 nm to 120 nm at a concentration of 11 million particles per mL (Bosman et al., 2005). Although the EST assay is based on mouse stem cells, we found weak embryotoxicity of the tested PS-nano and –micro. In contrast to the intestinal and placental models in this study, where no major impact on viability was found in the same concentration range, PS-micro were toxic for NIH/3 T3 and mES-cells from 25 µg/mL to 100 µg/mL. The result of weak embryotoxicity for both PS-nano and -micro can be explained by the relation of IC_{50} and ID_{50} values. The particles showed a slightly higher effect on differentiation (lower ID_{50}) compared to the toxicity (IC_{50}) of the tested material. In general, the EST assay is widely accepted (Campagnolo et al., 2013) and showed developmental toxicity for other particle types similar to what is reported in this study. This is the case for single-wall carbon nanotubes (Pietroiusti et al., 2011), cobalt ferrite nanoparticles coated with silanes and gold nanoparticles coated with hyaluronic acid (Di Guglielmo et al., 2010). Interestingly, silica nanoparticles had a stronger effect on development in the EST assay when smaller sizes were used, which is contrary to our findings (Park et al., 2009). Due to the environmental burden of nanoparticles, different studies investigated the effect on aquatic organisms. Asharani et al. found defects in cardiac development of zebrafish after exposure to silver and platinum, but not gold particles (Asharani et al., 2011). Della Torre et al., 2014 found no embryotoxicity for PS nanoparticles with carboxyl modification up to 50 µg/mL in sea urchin embryos (Della Torre et al., 2014).

Assessment of genotoxicity is another sensitive and essential parameter to address the toxic potential of nano- and microparticles. We concentrated on two cellular assays (p53 reporter gen assay and micronucleus assay) since the bacterial AMES test may not be suitable to assess the mutagenicity of nanosized materials (Clift et al., 2013; Drasler et al., 2017). They additionally suggest delaying the co-treatment with Cytochalasin-B (Cyt−B), which we did by implementing a 24 h co-culture period of PS-nano and PS-micro with cells prior to Cyt-B treatment. The micronucleus assay detects chromosome breakage and spindle interference, both leading to the formation of micronuclei. In line with our findings of an unaffected rate of micronuclei formation, previous studies also report no interference of COOH-PS-nano up to 5 µg/mL with the spindle apparatus (Liu et al., 2011). As genotoxicity can occur by several different pathways and mechanisms, an additional assay (p53 reporter gen assay) to identify DNA damaging factors was implemented. Nanomaterials can indirectly cause DNA damage through the generation of reactive oxidative species, a case especially often reported for metal-containing nanoparticles (Wang et al., 2017a). But, also nanoparticle coating can be attributed to DNA damage (Makama et al., 2018). Della Torre et al., 2014 found no p38 activation for PS nanoparticles with COOH surface modification, whereas NH_2-modified PS nanoparticles induced genotoxicity (Della Torre et al., 2014). Another aspect to DNA damage induction by PS-nano and PS-micro is the adsorption of mutagens due to their large relative surface area. It has been shown that PS nanoparticles could effectively bind hydrocarbons, many of them being classified as mutagens, under realistic *in vivo*

conditions (Liu et al., 2016). Although this aspect was beyond the scope of the current study, it highlights the relevance of genotoxicity assays using PS-nano and PS–micro.

In contrast to a single-organ study, the presented data on the effect of exactly the same type of PS-nano and PS- micro on multiple key endpoints *in vitro* provides a consistent data-set to compare organ-specific responses. This multi-organ, multi-endpoint study brings a great benefit to a more precise hazard assessment than investigating only one endpoint or one organ.

5. Conclusion

For a proper risk analysis of the emerging NP and MP, valid data for both, exposure and hazard, are needed. Our study presents a multi-organ and multi-endpoint toxicological assessment of PS nano- and microparticles. The results of our study bring a high added value in the field of MP bio-responses in humans and contribute to a better understanding of the potential mechanisms induced by NP and MP. This study gathered essential knowledge on the interaction, accumulation, translocation and specific effects caused by NP and MP in different tissues. Our study highlights that it is important to assess each tissue/cell type individually since the same material can induce distinct effects in different models. Thus, a combination of different assays, as well as specific standardized protocols for testing of plastics are needed for a more powerful predictive toxicological assessment of NP and MP in humans. Despite the fact that only minor acute toxic effects were observed in this study, there is still a need for further investigations of long-term effects of NP and MP. A better understanding of the relationships between translocation mechanisms and particle sizes would contribute very much to the risk evaluation of NP and MP in the environment.

Acknowledgements

This research is supported by funding from the German Federal Ministry for Education and Research (BMBF, 03X0150).

The authors would like to thank Prof. G. Desoye (Department of Obstetrics and Gynecology, Medical University Graz, Graz, Austria (with permission from Prof. P. Friedl, Institute of Biochemistry, Technical University Darmstadt, Darmstadt, Germany)) and Prof. Dr. Ursula Graf-Hausner (Zurich University of Applied Science (with permission from Dr. Alan L. Schwartz, Washington University School of Medicine, MO, USA)) for providing the HPEC-A2 and BeWo cells, respectively. The authors additionally thank Prof. Metka Filipic (National Institute of Biology, Ljubljana, Slovenia) for providing the HepG2CDKN1A–DsRed reporter gene cell line.

Author contributions

M.H., L.A., Y.K., B.E., and T.B. designed the study and wrote the original manuscript. M.H. and L.A. conducted all *in vitro* experiments regarding the intestine and the placenta, respectively. B.E. investigated potential genotoxicity and embryotoxicity. C.J. synthesized the particles. R.D. and F.M designed, conducted and evaluated the AF4 measurements. S.S. provided TEM images of the PS-nano and -micro. All authors were engaged in commenting on the manuscript and revised the manuscript.

Data availability

The data obtained/analysed during this study are available from the corresponding author on reasonable request.

Declaration of Competing Interest

The authors do not have any competing financial interests.

Appendix A. Supplementary data

Supplementary data to this article can be found online at https://doi.org/10.1016/j.tiv.2019.104610.

References

Plastic Soup Foundation, 2018. WWW Document. URL. https://www.plasticsoupfoundation.org/en/ (accessed 12.14.18).

Aardema, M.J., Snyder, R.D., Spicer, C., Divi, K., Morita, T., Mauthe, R.J., Gibson, D.P., Soelter, S., Curry, P.T., Thybaud, V., Lorenzon, G., Marzin, D., Lorge, E., 2006. SFTG international collaborative study on in vitro micronucleus test III. Using CHO cells. Mutat. Res. 607, 61–87. https://doi.org/10.1016/j.mrgentox.2006.04.002.

Adam, V., Caballero-Guzman, A., Nowack, B., 2018. Considering the forms of released engineered nanomaterials in probabilistic material flow analysis. Environ. Pollut. 243, 17–27. https://doi.org/10.1016/J.ENVPOL.2018.07.108.

Aengenheister, L., Keevend, K., Muoth, C., Schönenberger, R., Diener, L., Wick, P., Buerki-Thurnherr, T., 2018. An advanced human in vitro co-culture model for translocation studies across the placental barrier. Sci. Rep. 8, 1–12. https://doi.org/10.1038/s41598-018-23410-6.

Al-Jaibachi, R., Cuthbert, R.N., Callaghan, A., 2019. Examining effects of ontogenic microplastic transference on Culex mosquito mortality and adult weight. Sci. Total Environ. 651, 871–876. https://doi.org/10.1016/J.SCITOTENV.2018.09.236.

Asati, A., Santra, S., Kaittanis, C., Perez, J.M., 2010. Surface-charge-dependent cell localization and cytotoxicity of cerium oxide nanoparticles. ACS Nano 4, 5321–5331. https://doi.org/10.1021/nn100816s.

Asati, A., Santra, S., Kaittanis, C., Perez, J.M., 2011. Localization, surface-charge-dependent cell nanoparticles, cerium oxide. ACS Nano 4, 5321–5331. https://doi.org/10.1021/nn100816s.Surface-Charge-Dependent.

Asharani, P.V., lianwu, Y., Gong, Z., Valiyaveettil, S., 2011. Comparison of the toxicity of silver, gold and platinum nanoparticles in developing zebrafish embryos. Nanotoxicology 5, 43–54. https://doi.org/10.3109/17435390.2010.489207.

Ašmonaitė, G., Sundh, H., Asker, N., Carney Almroth, B., 2018. Rainbow trout maintain intestinal transport and barrier functions following exposure to polystyrene microplastics. Environ. Sci. Technol. 52, 14392–14401. https://doi.org/10.1021/acs.est.8b04848.

Auta, H.S., Emenike, C.U., Fauziah, S.H., 2017. Distribution and importance of microplastics in the marine environmentA review of the sources, fate, effects, and potential solutions. Environ. Int. 102, 165–176. https://doi.org/10.1016/j.envint.2017.02.013.

Avio, C.G., Gorbi, S., Regoli, F., 2017. Plastics and microplastics in the oceans: from emerging pollutants to emerged threat. Mar. Environ. Res. 128, 2–11. https://doi.org/10.1016/j.marenvres.2016.05.012.

Awet, T.T., Kohl, Y., Meier, F., Straskraba, S., Grün, A.L., Ruf, T., Jost, C., Drexel, R., Tunc, E., Emmerling, C., 2018. Effects of polystyrene nanoparticles on the microbiota and functional diversity of enzymes in soil. Environ. Sci. Eur. 30. https://doi.org/10.1186/s12302-018-0140-6.

Barboza, L.G.A., Dick Vethaak, A., Lavorante, B.R.B.O., Lundebye, A.K., Guilhermino, L., 2018. Marine microplastic debris: an emerging issue for food security, food safety and human health. Mar. Pollut. Bull. 133, 336–348. https://doi.org/10.1016/j.marpolbul.2018.05.047.

Bessa, F., Barría, P., Neto, J.M., Frias, J.P.G.L., Otero, V., Sobral, P., Marques, J.C., 2018. Occurrence of microplastics in commercial fish from a natural estuarine environment. Mar. Pollut. Bull. 128, 575–584. https://doi.org/10.1016/j.marpolbul.2018.01.044.

Betzer, O., Shilo, M., Opochinsky, R., Barnoy, E., Motiei, M., Okun, E., Yadid, G., Popovtzer, R., 2017. The effect of nanoparticle size on the ability to cross the blood–brain barrier: an *in vivo* study. Nanomedicine 12, 1533–1546. https://doi.org/10.2217/nnm-2017-0022.

Blagus, T., Zager, V., Cemazar, M., Sersa, G., Kamensek, U., Zegura, B., Nunic, J., Filipic, M., 2014. A cell-based biosensor system HepG2CDKN1A-DsRed for rapid and simple detection of genotoxic agents. Biosens. Bioelectron. 61, 102–111. https://doi.org/10.1016/j.bios.2014.05.002.

Blettler, M.C.M., Ulla, M.A., Rabuffetti, A.P., Garello, N., 2017. Plastic pollution in freshwater ecosystems: macro-, meso-, and microplastic debris in a floodplain lake. Environ. Monit. Assess. 189. https://doi.org/10.1007/s10661-017-6305-8.

Bosman, S.J., Nieto, S.P., Patton, W.C., Jacobson, J.D., Corselli, J.U., Chan, P.J., 2005. Development of mammalian embryos exposed to mixed-size nanoparticles. Clin. Exp. Obstet. Gynecol. 32, 222–224.

Bouwmeester, H., Hollman, P.C.H., Peters, R.J.B., 2015. Potential health impact of environmentally released micro- and nanoplastics in the human food production chain: experiences from nanotoxicology. Environ. Sci. Technol. 49, 8932–8947. https://doi.org/10.1021/acs.est.5b01090.

Browne, M.A., Niven, S.J., Galloway, T.S., Rowland, S.J., Thompson, R.C., 2013. Microplastic moves pollutants and additives to worms, reducing functions linked to health and biodiversity. Curr. Biol. 23, 2388–2392. https://doi.org/10.1016/j.cub.2013.10.012.

Burns, E.E., Boxall, A.B.A., 2018. Microplastics in the aquatic environment: evidence for or against adverse impacts and major knowledge gaps. Environ. Toxicol. Chem. 37, 2776–2796. https://doi.org/10.1002/etc.4268.

Campagnolo, L., Fenoglio, I., Massimiani, M., Magrini, A., Pietroiusti, A., 2013. Screening of nanoparticle embryotoxicity using embryonic stem cells. Methods Mol. Biol. (Clifton, N.J.) 49–60. https://doi.org/10.1007/7651_2013_11.

Canesi, L., Ciacci, C., Bergami, E., Monopoli, M.P., Dawson, K.A., Papa, S., Canonico, B., Corsi, I., 2015. Evidence for immunomodulation and apoptotic processes induced by

cationic polystyrene nanoparticles in the hemocytes of the marine bivalve Mytilus. Mar. Environ. Res. 111, 34–40. https://doi.org/10.1016/J.MARENVRES.2015.06.008.
Chiu, H.-W., Xia, T., Lee, Y.-H., Chen, C.-W., Tsai, J.-C., Wang, Y.-J., 2015. Cationic polystyrene nanospheres induce autophagic cell death through the induction of endoplasmic reticulum stress. Nanoscale 7, 736–746. https://doi.org/10.1039/c4nr05509h.
Clift, M.J.D., Raemy, D.O., Endes, C., Ali, Z., Lehmann, A.D., Brandenberger, C., Petri-Fink, A., Wick, P., Parak, W.J., Gehr, P., Schins, R.P.F., Rothen-Rutishauser, B., 2013. Can the Ames test provide an insight into nano-object mutagenicity? Investigating the interaction between nano-objects and bacteria. Nanotoxicology 7, 1373–1385. https://doi.org/10.3109/17435390.2012.741725.
Cole, M., Lindeque, P., Halsband, C., Galloway, T.S., 2011. Microplastics as contaminants in the marine environment: a review. Mar. Pollut. Bull. 62, 2588–2597. https://doi.org/10.1016/J.MARPOLBUL.2011.09.025.
Consultic, BKV, IK, VDMA, Bvse, Europe, P, 2016. Produktion, Verarbeitung und Verwertung von Kunststoffen in Deutschland 2015 -Kurzfassung.
Cuthbert, R.N., Al-Jaibachi, R., Dalu, T., Dick, J.T.A., Callaghan, A., 2019. The influence of microplastics on trophic interaction strengths and oviposition preferences of dipterans. Sci. Total Environ. 651, 2420–2423. https://doi.org/10.1016/J.SCITOTENV.2018.10.108.
Davidson, K., Dudas, S.E., 2016. Microplastic ingestion by wild and cultured Manila clams (Venerupis philippinarum) from Baynes sound, British Columbia. Arch. Environ. Contam. Toxicol. 71, 147–156. https://doi.org/10.1007/s00244-016-0286-4.
Della Torre, C., Bergami, E., Salvati, A., Faleri, C., Cirino, P., Dawson, K.A., Corsi, I., 2014. Accumulation and embryotoxicity of polystyrene nanoparticles at early stage of development of sea urchin embryos *Paracentrotus lividus*. Environ. Sci. Technol. 48, 12302–12311. https://doi.org/10.1021/es502569w.
Di Guglielmo, C., López, D.R., De Lapuente, J., Mallafre, J.M.L., Suàrez, M.B., 2010. Embryotoxicity of cobalt ferrite and gold nanoparticles: a first in vitro approach. Reprod. Toxicol. 30, 271–276. https://doi.org/10.1016/j.reprotox.2010.05.001.
Drasler, B., Sayre, P., Steinhäuser, K.G., Petri-Fink, A., Rothen-Rutishauser, B., 2017. In vitro approaches to assess the hazard of nanomaterials. NanoImpact 8, 99–116. https://doi.org/10.1016/J.IMPACT.2017.08.002.
Efimova, I., Bagaeva, M., Bagaev, A., Kileso, A., Chubarenko, I.P., 2018. Secondary microplastics generation in the sea swash zone with coarse bottom sediments: laboratory experiments. Front. Mar. Sci. 5. https://doi.org/10.3389/fmars.2018.00313.
EFSA, 2016a. Presence of microplastics and nanoplastics in food, with particular focus on seafood. EFSA J. 14. https://doi.org/10.2903/j.efsa.2016.4501.
EFSA, 2016b. Presence of microplastics and nanoplastics in food, with particular focus on seafood. EFSA J. 14. https://doi.org/10.2903/j.efsa.2016.4501.
Ekvall, M.T., Lundqvist, M., Kelpsiene, E., Šileikis, E., Gunnarsson, S.B., Cedervall, T., 2019. Nanoplastics formed during the mechanical breakdown of daily-use polystyrene products. Nanoscale Adv. 1, 1055–1061. https://doi.org/10.1039/c8na00210j.
European Commission, 2018. Directive of the European Parliament and the Council on the Reduction of the Impact of Certain Plastic Products on the Environment (2018/0172). (doi:COM(2018) 340 final 2018/0172 (COD)).
Fernandes, T., Cristofi, N., Stone, V., 2007. The Environmental Implications of Nanomaterials.
Fischer, D., Li, Y., Ahlemeyer, B., Krieglstein, J., Kissel, T., 2003. In vitro cytotoxicity of polycations: influence of polymer structure on cell viability and hemolysis. Biomaterials 24, 1121–1131. https://doi.org/10.1016/S0142-9612(02)00445-3.
Fischer, E.K., Paglialonga, L., Czech, E., Tamminga, M., 2016. Microplastic pollution in lakes and lake shoreline sediments – a case study on Lake Bolsena and Lake Chiusi (central Italy). Environ. Pollut. 213, 648–657. https://doi.org/10.1016/j.envpol.2016.03.012.
Fröhlich, E., Meindl, C., Roblegg, E., Ebner, B., Absenger, M., Pieber, T.R., 2012. Action of polystyrene nanoparticles of different sizes on lysosomal function and integrity. Part. Fibre Toxicol. 9, 26. https://doi.org/10.1186/1743-8977-9-26.
Gall, S.C., Thompson, R.C., 2015. The impact of debris on marine life. Mar. Pollut. Bull. 92, 170–179. https://doi.org/10.1016/j.marpolbul.2014.12.041.
Galloway, T.S., Cole, M., Lewis, C., 2017. Interactions of microplastic debris throughout the marine ecosystem. Nat. Ecol. Evol. 1, 0116. https://doi.org/10.1038/s41559-017-0116.
Gewert, B., Plassmann, M.M., Macleod, M., 2015. Pathways for degradation of plastic polymers floating in the marine environment. Environ. Sci. Process. Impacts 17, 1513–1521. https://doi.org/10.1039/c5em00207a.
Geyer, R., Jambeck, J.R., Law, K.L., 2017. Production, use, and fate of all plastics ever made. Sci. Adv. 3, e1700782. https://doi.org/10.1126/sciadv.1700782.
Grafmueller, S., Manser, P., Diener, L., Diener, P.-A., Maeder-Althaus, X., Maurizi, L., Jochum, W., Krug, H.F., Buerki-Thurnherr, T., von Mandach, U., Wick, P., 2015. Bidirectional transfer study of polystyrene nanoparticles across the placental barrier in an ex vivo human placental perfusion model. Environ. Health Perspect. 123, 1280–1286. https://doi.org/10.1289/ehp.1409271.
Harush-Frenkel, O., Bivas-Benita, M., Nassar, T., Springer, C., Sherman, Y., Avital, A., Altschuler, Y., Borlak, J., Benita, S., 2010. A safety and tolerability study of differently-charged nanoparticles for local pulmonary drug delivery. Toxicol. Appl. Pharmacol. 246, 83–90. https://doi.org/10.1016/J.TAAP.2010.04.011.
Hermsen, E., Pompe, R., Besseling, E., Koelmans, A.A., 2017. Detection of low numbers of microplastics in North Sea fish using strict quality assurance criteria. Mar. Pollut. Bull. 122, 253–258. https://doi.org/10.1016/j.marpolbul.2017.06.051.
Holm, P., Schulz, G., Athanasopulu, K., 2013. Meeresverschmutzung der neuen Art: Mikroplastik - ein unsichtbarer Störenfried. Biol. Unserer Zeit 43, 27–33. https://doi.org/10.1002/biuz.201310497.
Huerta Lwanga, E., Gertsen, H., Gooren, H., Peters, P., Salánki, T., van der Ploeg, M., Besseling, E., Koelmans, A.A., Geissen, V., 2017. Incorporation of microplastics from litter into burrows of Lumbricus terrestris. Environ. Pollut. 220, 523–531. https://doi.org/10.1016/J.ENVPOL.2016.09.096.
Hughes, J.M., Budd, P.M., Grieve, A., Dutta, P., Tiede, K., Lewis, J., 2015. Highly monodisperse, lanthanide-containing polystyrene nanoparticles as potential standard reference materials for environmental "nano" fate analysis. J. Appl. Polym. Sci. 132. https://doi.org/10.1002/app.42061.
Hussain, N., Jaitley, V., Florence, A.T., 2001. Recent advances in the understanding of uptake of microparticulates across the gastrointestinal lymphatics. Adv. Drug Deliv. Rev. 50, 107–142. https://doi.org/10.1016/S0169-409X(01)00152-1.
Iñiguez, M.E., Conesa, J.A., Fullana, A., 2017. Microplastics in Spanish table salt. Sci. Rep. 7, 8620. https://doi.org/10.1038/s41598-017-09128-x.
Isobe, A., 2016. Percentage of microbeads in pelagic microplastics within Japanese coastal waters. Mar. Pollut. Bull. 110, 432–437. https://doi.org/10.1016/j.marpolbul.2016.06.030.
Ivar do Sul, J.A., Costa, M.F., 2014. The present and future of microplastic pollution in the marine environment. Environ. Pollut. 185, 352–364. https://doi.org/10.1016/J.ENVPOL.2013.10.036.
Jambeck, J.R., Geyer, R., Wilcox, C., Siegler, T.R., Perryman, M., Andrady, A., Narayan, R., Law, K.L., 2015. Marine pollution. Plastic waste inputs from land into the ocean. Science 347, 768–771. https://doi.org/10.1126/science.1260352.
Juliano, C., Magrini, G., 2017. Cosmetic ingredients as emerging pollutants of environmental and health concern. A mini-review. Cosmetics 4, 11. https://doi.org/10.3390/cosmetics4020011.
Kanhai, L.D.K., Officer, R., Lyashevska, O., Thompson, R.C., O'Connor, I., 2017. Microplastic abundance, distribution and composition along a latitudinal gradient in the Atlantic Ocean. Mar. Pollut. Bull. 115, 307–314. https://doi.org/10.1016/j.marpolbul.2016.12.025.
Karami, A., Golieskardi, A., Keong Choo, C., Larat, V., Galloway, T.S., Salamatinia, B., 2017. Corrigendum: the presence of microplastics in commercial salts from different countries (Scientific Reports (2017) 7 (46173) DOI: 10.1038/srep46173). Sci. Rep. 7, 1–11. https://doi.org/10.1038/srep46838.
Karami, A., Golieskardi, A., Choo, C.K., Larat, V., Karbalaei, S., Salamatinia, B., 2018. Microplastic and mesoplastic contamination in canned sardines and sprats. Sci. Total Environ. 612, 1380–1386. https://doi.org/10.1016/j.scitotenv.2017.09.005.
Kawecki, D., Scheeder, P.R.W., Nowack, B., 2018. Probabilistic material flow analysis of seven commodity plastics in Europe. Environ. Sci. Technol. 52, 9874–9888. https://doi.org/10.1021/acs.est.8b01513.
Klein, S., Worch, E., Knepper, T.P., 2015. Occurrence and spatial distribution of microplastics in river shore sediments of the Rhine-Main area in Germany. Environ. Sci. Technol. 49, 6070–6076. https://doi.org/10.1021/acs.est.5b00492.
Kloet, S.K., Walczak, A.P., Louisse, J., van den Berg, H.H.J., Bouwmeester, H., Tromp, P., Fokkink, R.G., Rietjens, I.M.C.M., 2015. Translocation of positively and negatively charged polystyrene nanoparticles in an in vitro placental model. Toxicol. in Vitro 29, 1701–1710. https://doi.org/10.1016/J.TIV.2015.07.003.
Kosuth, M., Mason, S.A., Wattenberg, E.V., 2018. Anthropogenic contamination of tap water, beer, and sea salt. PLoS One 13, e0194970. https://doi.org/10.1371/journal.pone.0194970.
Kreyling, W.G., Holzwarth, U., Haberl, N., Kozempel, J., Hirn, S., Wenk, A., Schleh, C., Schäffler, M., Lipka, J., Semmler-Behnke, M., Gibson, N., 2017. Quantitative biokinetics of titanium dioxide nanoparticles after intravenous injection in rats: part 1. Nanotoxicology 11, 434–442. https://doi.org/10.1080/17435390.2017.1306892.
Kulkarni, S.A., Feng, S.S., 2013. Effects of particle size and surface modification on cellular uptake and biodistribution of polymeric nanoparticles for drug delivery. Pharm. Res. 30, 2512–2522. https://doi.org/10.1007/s11095-012-0958-3.
Lambert, S., Wagner, M., 2016. Characterisation of nanoplastics during the degradation of polystyrene. Chemosphere 145, 265–268. https://doi.org/10.1016/j.chemosphere.2015.11.078.
Law, K.L., Thompson, R.C., 2014. Microplastics in the seas. Science (80-.) 345, 144–145. https://doi.org/10.1126/science.1254065.
Lechner, A., Keckeis, H., Lumesberger-Loisl, F., Zens, B., Krusch, R., Tritthart, M., Glas, M., Schludermann, E., 2014. The Danube so colourful: a potpourri of plastic litter outnumbers fish larvae in Europe's second largest river. Environ. Pollut. 188, 177–181. https://doi.org/10.1016/j.envpol.2014.02.006.
Lehner, R., Weder, C., Petri-Fink, A., Rothen-Rutishauser, B., 2019. Emergence of nanoplastic in the environment and possible impact on human health. Environ. Sci. Technol. 53, 1748–1765. https://doi.org/10.1021/acs.est.8b05512.
Leslie, H.A., 2014. Review of microplastics in cosmetics : scientific background on a potential source of plastic particulate marine litter to support decision-making, report R14/29. IVM Institute for Environmental Studies, Amsterdam.
Li, W.C., Tse, H.F., Fok, L., 2016. Plastic waste in the marine environment: a review of sources, occurrence and effects. Sci. Total Environ. 566–567, 333–349. https://doi.org/10.1016/j.scitotenv.2016.05.084.
Liebezeit, G., Liebezeit, E., 2013. Non-pollen particulates in honey and sugar. Food Addit. Contam. A 30, 2136–2140. https://doi.org/10.1080/19440049.2013.843025.
Liebezeit, G., Liebezeit, E., 2014. Synthetic particles as contaminants in German beers. Food Addit. Contam. A 31, 1574–1578. https://doi.org/10.1080/19440049.2014.945099.
Liu, Yuexian, Li, W., Lao, F., Liu, Ying, Wang, L., Bai, R., Zhao, Y., Chen, C., 2011. Intracellular dynamics of cationic and anionic polystyrene nanoparticles without direct interaction with mitotic spindle and chromosomes. Biomaterials 32, 8291–8303. https://doi.org/10.1016/J.BIOMATERIALS.2011.07.037.
Liu, L., Fokkink, R., Koelmans, A.A., 2016. Sorption of polycyclic aromatic hydrocarbons to polystyrene nanoplastic. Environ. Toxicol. Chem. 35, 1650–1655. https://doi.org/10.1002/etc.3311.
Loos, C., Syrovets, T., Musyanovych, A., Mailänder, V., Landfester, K., Nienhaus, G.U.,

Simmet, T., 2014. Functionalized polystyrene nanoparticles as a platform for studying bio–nano interactions. Beilstein J. Nanotechnol. 5, 2403–2412. https://doi.org/10.3762/bjnano.5.250.

Luís, L.G., Ferreira, P., Fonte, E., Oliveira, M., Guilhermino, L., 2015. Does the presence of microplastics influence the acute toxicity of chromium(VI) to early juveniles of the common goby (Pomatoschistus microps)? A study with juveniles from two wild estuarine populations. Aquat. Toxicol. 164, 163–174. https://doi.org/10.1016/J.AQUATOX.2015.04.018.

Lusher, A.L., Tirelli, V., O'Connor, I., Officer, R., 2015. Microplastics in Arctic polar waters: the first reported values of particles in surface and sub-surface samples. Sci. Rep. 5, 14947. https://doi.org/10.1038/srep14947.

Lusher, A., Hollman, P., Mandoza-Hill, J.J., 2017. Microplastics in Fisheries and Aquaculture, FAO Fisheries and Aquaculture Technical Paper.

Makama, S., Kloet, S.K., Piella, J., van den Berg, H., de Ruijter, N.C.A., Puntes, V.F., Rietjens, I.M.C.M., van den Brink, N.W., 2018. Effects of systematic variation in size and surface coating of silver nanoparticles on their in vitro toxicity to macrophage RAW 264.7 cells. Toxicol. Sci. 162, 79–88. https://doi.org/10.1093/toxsci/kfx228.

Miklos, D., Obermaier, N., Jekel, M., 2016. Mikroplastik: Entwicklung eines Umweltbewertungskonzepts: Erste Überlegungen zur Relevanz von synthetischen Polymeren in der Umwelt.

Mintenig, Löder, Gerdts, 2014. Mikroplastik in Trinkwasser Untersuchung im Trinkwasserversorgungsgebiet des Oldenburgisch-Ostfriesischen Wasserverbandes (OOWV) in Niedersachsen Probenanalyse mittels Mikro-FTIR Spektroskopie [WWW Document].

von Moos, N., Burkhardt-Holm, P., Köhler, A., 2012. Uptake and effects of microplastics on cells and tissue of the blue mussel Mytilus edulis L. after an experimental exposure. Environ. Sci. Technol. 46, 11327–11335. https://doi.org/10.1021/es302332w.

Park, M.V.D.Z., Annema, W., Salvati, A., Lesniak, A., Elsaesser, A., Barnes, C., McKerr, G., Howard, C.V., Lynch, I., Dawson, K.A., Piersma, A.H., de Jong, W.H., 2009. In vitro developmental toxicity test detects inhibition of stem cell differentiation by silica nanoparticles. Toxicol. Appl. Pharmacol. 240, 108–116. https://doi.org/10.1016/j.taap.2009.07.019.

Pietroiusti, A., Massimiani, M., Fenoglio, I., Colonna, M., Valentini, F., Palleschi, G., Camaioni, A., Magrini, A., Siracusa, G., Bergamaschi, A., Sgambato, A., Campagnolo, L., 2011. Low doses of pristine and oxidized single-wall carbon nanotubes affect mammalian embryonic development. ACS Nano 5, 4624–4633. https://doi.org/10.1021/nn200372g.

PlasticsEurope, 2015. Plastics - the facts 2015. An analysis of European plastics production, demand and waste data. Plast. (the Assoc. Plast. Manifacturers Eur.) 1–30. https://doi.org/10.1016/j.marpolbul.2013.01.015.

PlasticsEurope, 2017. Plastics – The Facts 2017. https://doi.org/10.1016/j.marpolbul.2013.01.015.

Pörschke, S., Eloo, C., 2016. Ersatz von Mikroplastik in kosmetischen Produkten. Chemie-Ingenieur-Technik 874–880. https://doi.org/10.1002/cite.201500156.

Prata, J.C., 2018. Airborne microplastics: consequences to human health? Environ. Pollut. 234, 115–126. https://doi.org/10.1016/j.envpol.2017.11.043.

Revel, M., Châtel, A., Mouneyrac, C., 2018. Micro(nano)plastics: a threat to human health? Curr. Opin. Environ. Sci. Heal. 1, 17–23. https://doi.org/10.1016/j.coesh.2017.10.003.

Rodriguez-Seijo, A., Lourenço, J., Rocha-Santos, T.A.P., da Costa, J., Duarte, A.C., Vala, H., Pereira, R., 2017. Histopathological and molecular effects of microplastics in Eisenia andrei Bouché. Environ. Pollut. 220, 495–503. https://doi.org/10.1016/j.envpol.2016.09.092.

Rummel, C.D., Löder, M.G.J., Fricke, N.F., Lang, T., Griebeler, E.M., Janke, M., Gerdts, G., 2016. Plastic ingestion by pelagic and demersal fish from the North Sea and Baltic Sea. Mar. Pollut. Bull. 102, 134–141. https://doi.org/10.1016/j.marpolbul.2015.11.043.

Schimpel, C., Teubl, B., Absenger, M., Meindl, C., Fröhlich, E., Leitinger, G., Zimmer, A., Roblegg, E., 2014. Development of an advanced intestinal in vitro triple culture permeability model to study transport of nanoparticles. Mol. Pharm. 11, 808–818. https://doi.org/10.1021/mp400507g.

Schirinzi, G.F., Pérez-Pomeda, I., Sanchís, J., Rossini, C., Farré, M., Barceló, D., 2017. Cytotoxic effects of commonly used nanomaterials and microplastics on cerebral and epithelial human cells. Environ. Res. 159, 579–587. https://doi.org/10.1016/j.envres.2017.08.043.

Schmidt, C., Lautenschlaeger, C., Collnot, E.-M., Schumann, M., Bojarski, C., Schulzke, J.-D., Lehr, C.-M., Stallmach, A., 2013. Nano- and microscaled particles for drug targeting to inflamed intestinal mucosa—a first in vivo study in human patients. J. Control. Release 165, 139–145. https://doi.org/10.1016/J.JCONREL.2012.10.019.

Seiler, A.E.M., Spielmann, H., 2011. The validated embryonic stem cell test to predict embryotoxicity in vitro. Nat. Protoc. 6, 961–978. https://doi.org/10.1038/nprot.2011.348.

Shim, W.J., Hong, S.H., Eo, S., 2018. Marine microplastics: Abundance, distribution, and composition. In: Microplastic Contamination in Aquatic Environments. Elsevier. https://doi.org/10.1016/B978-0-12-813747-5.00001-1.

Smith, M., Love, D.C., Rochman, C.M., Neff, R.A., 2018. Microplastics in seafood and the implications for human health. Curr. Environ. Heal. Rep. 5, 375–386. https://doi.org/10.1007/s40572-018-0206-z.

de Souza Machado, A.A., Kloas, W., Zarfl, C., Hempel, S., Rillig, M.C., 2018. Microplastics as an emerging threat to terrestrial ecosystems. Glob. Chang. Biol. 24, 1405–1416. https://doi.org/10.1111/gcb.14020.

Suaria, G., Avio, C.G., Mineo, A., Lattin, G.L., Magaldi, M.G., Belmonte, G., Moore, C.J., Regoli, F., Aliani, S., 2016. The mediterranean plastic soup: synthetic polymers in mediterranean surface waters. Sci. Rep. 6, 37551. https://doi.org/10.1038/srep37551.

Sun, X., Chen, B., Li, Q., Liu, N., Xia, B., Zhu, L., Qu, K., 2018. Toxicities of polystyrene nano- and microplastics toward marine bacterium Halomonas alkaliphila. Sci. Total Environ. 642, 1378–1385. https://doi.org/10.1016/J.SCITOTENV.2018.06.141.

Tanaka, K., Takada, H., 2016. Microplastic fragments and microbeads in digestive tracts of planktivorous fish from urban coastal waters. Sci. Rep. 6, 1–8. https://doi.org/10.1038/srep34351.

Tenzer, S., Docter, D., Kuharev, J., Musyanovych, A., Fetz, V., Hecht, R., Schlenk, F., Fischer, D., Kiouptsi, K., Reinhardt, C., Landfester, K., Schild, H., Maskos, M., Knauer, S.K., Stauber, R.H., 2013. Rapid formation of plasma protein corona critically affects nanoparticle pathophysiology. Nat. Nanotechnol. 8, 772–781. https://doi.org/10.1038/nnano.2013.181.

Teubl, B.J., Meindl, C., Eitzlmayr, A., Zimmer, A., Fröhlich, E., Roblegg, E., 2013. In-vitro permeability of neutral polystyrene particles via buccal mucosa. Small 9, 457–466. https://doi.org/10.1002/smll.201201789.

Van Cauwenberghe, L., Janssen, C.R., 2014. Microplastics in bivalves cultured for human consumption. Environ. Pollut. 193, 65–70. https://doi.org/10.1016/j.envpol.2014.06.010.

Van Cauwenberghe, L., Claessens, M., Vandegehuchte, M.B., Janssen, C.R., 2015. Microplastics are taken up by mussels (Mytilus edulis) and lugworms (Arenicola marina) living in natural habitats. Environ. Pollut. 199, 10–17. https://doi.org/10.1016/j.envpol.2015.01.008.

Vandenberg, L.N., Colborn, T., Hayes, T.B., Heindel, J.J., Jacobs, D.R., Lee, D.H., Shioda, T., Soto, A.M., vom Saal, F.S., Welshons, W.V., Zoeller, R.T., Myers, J.P., 2012. Hormones and endocrine-disrupting chemicals: low-dose effects and nonmonotonic dose responses. Endocr. Rev. 33, 378–455. https://doi.org/10.1210/er.2011-1050.

Vroom, R.J.E., Koelmans, A.A., Besseling, E., Halsband, C., 2017. Aging of microplastics promotes their ingestion by marine zooplankton. Environ. Pollut. 231, 987–996. https://doi.org/10.1016/j.envpol.2017.08.088.

Walczak, A.P., Kramer, E., Hendriksen, P.J.M., Tromp, P., Helsper, J.P.F.G., van der Zande, M., Rietjens, I.M.C.M., Bouwmeester, H., 2015. Translocation of differently sized and charged polystyrene nanoparticles in *in vitro* intestinal cell models of increasing complexity. Nanotoxicology 9, 453–461. https://doi.org/10.3109/17435390.2014.944599.

Waller, C.L., Griffiths, H.J., Waluda, C.M., Thorpe, S.E., Loaiza, I., Moreno, B., Pacherres, C.O., Hughes, K.A., 2017. Microplastics in the Antarctic marine system: an emerging area of research. Sci. Total Environ. 598, 220–227. https://doi.org/10.1016/j.scitotenv.2017.03.283.

Wang, J., Tan, Z., Peng, J., Qiu, Q., Li, M., 2016. The behaviors of microplastics in the marine environment. Mar. Environ. Res. 113, 7–17. https://doi.org/10.1016/j.marenvres.2015.10.014.

Wang, E., Huang, Y., Du, Q., Sun, Y., 2017a. Silver nanoparticle induced toxicity to human sperm by increasing ROS(reactive oxygen species) production and DNA damage. Environ. Toxicol. Pharmacol. 52, 193–199. https://doi.org/10.1016/J.ETAP.2017.04.010.

Wang, W., Ndungu, A.W., Li, Z., Wang, J., 2017b. Microplastics pollution in inland freshwaters of China: a case study in urban surface waters of Wuhan, China. Sci. Total Environ. 575, 1369–1374. https://doi.org/10.1016/J.SCITOTENV.2016.09.213.

Wang, Y., Zhang, D., Zhang, M., Mu, J., Ding, G., Mao, Z., Cao, Y., Jin, F., Cong, Y., Wang, L., Zhang, W., Wang, J., 2019. Effects of ingested polystyrene microplastics on brine shrimp, Artemia parthenogenetica. Environ. Pollut. 244, 715–722. https://doi.org/10.1016/j.envpol.2018.10.024.

Waring, R.H., Harris, R.M., Mitchell, S.C., 2018. Plastic contamination of the food chain: a threat to human health? Maturitas 115, 64–68. https://doi.org/10.1016/J.MATURITAS.2018.06.010.

Watts, A.J.R., Urbina, M.A., Corr, S., Lewis, C., Galloway, T.S., 2015. Ingestion of plastic microfibers by the crab *Carcinus maenas* and its effect on food consumption and energy balance. Environ. Sci. Technol. 49, 14597–14604. https://doi.org/10.1021/acs.est.5b04026.

Watts, A.J.R., Urbina, M.A., Goodhead, R., Moger, J., Lewis, C., Galloway, T.S., 2016. Effect of microplastic on the gills of the shore crab *Carcinus maenas*. Environ. Sci. Technol. 50, 5364–5369. https://doi.org/10.1021/acs.est.6b01187.

Welden, N.A.C., Cowie, P.R., 2016. Long-term microplastic retention causes reduced body condition in the langoustine, Nephrops norvegicus. Environ. Pollut. 218, 895–900. https://doi.org/10.1016/J.ENVPOL.2016.08.020.

Wick, P., Malek, A., Manser, P., Meili, D., Maeder-Althaus, X., Diener, L., Diener, P.-A., Zisch, A., Krug, H.F., von Mandach, U., 2010. Barrier capacity of human placenta for nanosized materials. Environ. Health Perspect. 118, 432–436. https://doi.org/10.1289/ehp.0901200.

Woodall, L.C., Sanchez-Vidal, A., Canals, M., Paterson, G.L.J., Coppock, R., Sleight, V., Calafat, A., Rogers, A.D., Narayanaswamy, B.E., Thompson, R.C., 2014. The deep sea is a major sink for microplastic debris. R. Soc. open Sci. 1, 140317. https://doi.org/10.1098/rsos.140317.

Wright, S.L., Kelly, F.J., 2017. Plastic and human health: a micro issue? Environ. Sci. Technol. 51, 6634–6647. https://doi.org/10.1021/acs.est.7b00423.

Wright, S.L., Thompson, R.C., Galloway, T.S., 2013. The physical impacts of microplastics on marine organisms: a review. Environ. Pollut. 178, 483–492. https://doi.org/10.1016/J.ENVPOL.2013.02.031.

Yang, D., Shi, H., Li, L., Li, J., Jabeen, K., Kolandhasamy, P., 2015. Microplastic pollution in table salts from China. Environ. Sci. Technol. 49, 13622–13627. https://doi.org/10.1021/acs.est.5b03163.